Hillslope-scale exploration of the relative contribution of base flow, seepage flow and overland flow to streamflow dynamics

Nicolas Cornette, Clément Roques, Alexandre Boisson, Quentin Courtois, Jean Marçais, Josette Launay, Guillaume Pajot, Florence Habets, Jean-Raynald de Dreuzy

Journal Pre-proofs

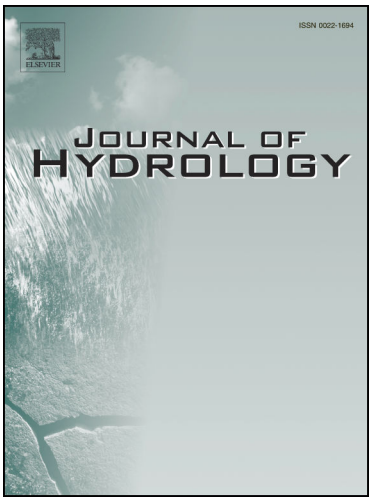

Research papers

Hillslope-scale exploration of the relative contribution of base flow, seepage flow and overland flow to streamflow dynamics

Nicolas Cornette, Clément Roques, Alexandre Boisson, Quentin Courtois, Jean Marçais, Josette Launay, Guillaume Pajot, Florence Habets, Jean-Raynald de Dreuzy

PII: S0022-1694(22)00567-4
DOI: https://doi.org/10.1016/j.jhydrol.2022.127992
Reference: HYDROL 127992

To appear in: *Journal of Hydrology*

Received Date: 16 December 2021
Revised Date: 19 May 2022
Accepted Date: 23 May 2022

Please cite this article as: Cornette, N., Roques, C., Boisson, A., Courtois, Q., Marçais, J., Launay, J., Pajot, G., Habets, F., de Dreuzy, J-R., Hillslope-scale exploration of the relative contribution of base flow, seepage flow and overland flow to streamflow dynamics, *Journal of Hydrology* (2022), doi: https://doi.org/10.1016/j.jhydrol.2022.127992

Hillslope-scale exploration of the relative contribution of base flow, seepage flow and overland flow to streamflow dynamics

Nicolas Cornette[1,2*], Clément Roques[1,3], Alexandre Boisson[2], Quentin Courtois[1], Jean Marçais[4], Josette Launay[5], Guillaume Pajot[5,6], Florence Habets[7], Jean-Raynald de Dreuzy[1,6]

[1] Univ Rennes, CNRS, Géosciences Rennes - UMR 6118, F-35000 Rennes, France

[2] BRGM - DAT Bretagne, Rennes, France

[3] Centre for Hydrology and Geothermics (CHYN), Université de Neuchâtel, Neuchâtel, Switzerland

[4] INRAE, UR Riverly, F-69625 Villeurbanne, France

[5] CRESEB, Rennes, France

[6] Univ Rennes, CNRS, OSUR - UMS 3343, F-35000 Rennes, France

[7] CNRS UMR 8538, Laboratoire de Géologie, École Normale Supérieure, PSL Research University, 75005 Paris, France

Corresponding Author**:** Nicolas Cornette (nicolas.cornette@univ-rennes1.fr)

Keywords: Hillslope-scale, groundwater-surface water interactions, Boussinesq, equivalent hillslope, seepage flow

Highlights:

- Groundwater-surface water interactions are studied in two shallow aquifers
- A combination of hillslope processes shapes the catchment-scale streamflows.

- Low-conductive hillslopes enhance overland flows and sustain late recessions.
- High-diffusive hillslopes shape the event- and seasonal-scale recessions.
- Hydraulic properties are significantly heterogeneous at the catchment scale.

Abstract

Surface and subsurface flows interact at different spatial and temporal scales through the development of saturated areas occurring when the aquifer reaches the surface. While this interaction exerts a strong control in the partitioning of water between base flow, seepage flow and overland flow, its quantification remains a challenge. Here, we propose a novel modeling approach based on two equivalent hillslopes to capture spatial and temporal variabilities of the main processes. We calibrate their subsurface hydraulic properties based on the temporal dynamics of stream discharge. The model is tested on two pilot catchments located in Brittany (France). For both catchments, the model is successfully calibrated on 40 years of stream discharge data. The results demonstrate that contrasted hydraulic properties are required, with: (1) a relatively low conductive hillslope (conductivities between $3x10^{-8}$ m/s and $2x10^{-6}$ m/s) enhancing overland flows during recharge periods while also sustaining low flows in the late recession period through slow aquifer discharge, and (2) a highly diffusive hillslope (diffusivity between $5x10^{-3}$ m^2/s and $3x10^{-1}$ m^2/s) dominantly shaping the event- to seasonal-scale streamflow recession behavior. The strong contrast of the two hillslopes reveals the fundamental role of heterogeneity in controlling groundwater storage-discharge functions, ruling out any homogeneous equivalent at the catchment scale. Low flows appear to be a non-obvious combination of the contributions of the two hillslopes, the less diffusive hillslope catching up to the more conductive one by the end of the low flow period. Catchment-scale responses integrate complex interactions between recharge, groundwater and overland flows through the volume of subsurface storage and the extent of the saturated area.

1. INTRODUCTION

At the regional to continental scale, the feedback mechanisms between climate, groundwater storage and stream discharge dynamics are critical in controlling flow partitioning within the water cycle (Abbott et al., 2019; Anderson and Burt, 1978; Hewlett and Hibbert, 1967; Sophocleous, 2002). At the local streambed scale, these feedbacks are also key in the regulation of processes by enhancing biogeochemical activities through the mixing of different water types (Bartsch et al., 2014; Chae et al., 2006; Hyun et al., 2011). At the intermediary hillslope to catchment scales, they are also critical since the intersection of the groundwater table with the topography leads to the discharge of subsurface water and controls the emergence of the surface stream and wetland networks (Devauchelle et al., 2012; Dunne and Black, 1970; Messager et al., 2021). At the surface, groundwater seepage occurs under a variety of hydrogeological conditions such as low relief, limited aquifer depth, low hydraulic conductivity and porosity or when average recharge rates are significantly high with respect to aquifer transmissivity (Condon and Maxwell, 2015; Gleeson et al., 2011a; Haitjema and Mitchell-Bruker, 2005; Price, 2011). Such conditions have been found in numerous settings from the crystalline regions under temperate or cold climates (Dewandel et al., 2021; Kolbe et al., 2016, 2020; Wyns et al., 2004) to the glaciated headwater catchments (Devito et al., 1996) or the clay areas with undulating landscapes (Dahl et al., 2007). Groundwater-surface water interactions thus appear to be mainly shaped by the relative depth of the water table with respect to the geomorphic features of the landscape (Bresciani et al., 2014; Gleeson and Manning, 2008; Haitjema and Mitchell-Bruker, 2005).

Even though these interactions are well identified, groundwater and surface water processes have mostly been handled independently at the hillslope to catchment scales (Staudinger et al.,

2019). For example, the analysis of streamflow recessions has extensively been used to estimate hydraulic properties of the groundwater system assuming that overland flows can be neglected in low-flow periods. Analytical solutions are derived from the integration of simplified hillslope configurations neglecting surface-groundwater interactions (Brutsaert and Nieber, 1977). Relations between groundwater storage and stream discharge dynamics have been further extended with transfer functions (Kirchner, 2009). Similarly, models relying on interconnected reservoirs (Perrin et al., 2001) consider such interactions through the transfer of water between both surface and subsurface reservoirs where the fluxes are dependent on the subsurface storage and an exchange coefficient. Surface-groundwater interactions are, however, more complex than a first-order reservoir overflow. They imply spatial and temporal evolutions also driven by the variations of the saturated areas. At the hillslope scale, contribution of aquifers to stream discharge is typically composed of: i) fast groundwater transfers through shallow soil or highly permeable lithological units; ii) slow groundwater flow, mainly influencing baseflow regimes and; iii) fast saturation-excess overland flows (Brutsaert, 2005). The partitioning between these slow and fast flow components is controlled by the precipitations rates, the intensity of the seepage flow, and more fundamentally, by the depth and gradient of the groundwater table. Groundwater seepage and saturated areas occur at specific locations along the hillslope, typically emerging downslope, near the main stream channel (Dunne and Black, 1970). They can also develop after steep slopes (Kolbe et al., 2016), downhill of plateaus with low hydraulic conductivities (Bresciani et al., 2014; Ogden and Watts, 2000), or be induced by convergent geomorphology (Aryal et al., 2002, 2003; Paniconi et al., 2003). They occur predominantly in wet conditions, even though some of them may remain active during extended dry periods due to steady groundwater inputs (Ala-aho et al., 2017). An important scientific challenge remains to represent such key processes involved at the surface-subsurface interface both at the catchment and the regional scales and quantify their relative contribution (Blöschl et al., 2019).

While global scale climate and land surface models give the major trends of atmospheric and surface processes, they cannot go down to the hillslope scale (Fan et al., 2019; Xiao et al., 2019).

We therefore aim at studying the impact of these hillslope processes on streamflow dynamics by modeling two pilot catchments in Brittany (France) where poorly permeable and shallow aquifers within low-relief landscapes lead to the emergence of dense networks of streams and wetlands well connected to the groundwater system (Dewandel et al., 2021; Franks et al., 1998; Gascuel-Odoux et al., 2010). We use stream discharge time series to inform the hillslope model designed to capture the combination of processes and quantify their relative contributions. We consider an equivalent hillslope model to quantify the temporal dynamics of surface-subsurface interactions. The assumption of considering hillslope as the representative elementary scale to describe the dominant processes is supported by the strong hillslope organization of groundwater and seepage flow typical of lowland crystalline basement regions (Fan et al., 2019; Kolbe et al., 2016; Loritz et al., 2017). With this approach, we also aim at identifying the first-order geomorphological and geological controls on streamflow dynamics. A better understanding of the processes and their relative contributions to the temporal dynamics of streamflow is essential for the management of water resources, which, to date, mostly relies on empirical data, sparse observations and simplified models to predict catchment-scale responses to climate forcing (Fangmann and Haberlandt, 2019). The need for accurate predictions is even reinforced in the perspective of global changes (Famiglietti, 2014). The parsimonious approach proposed in this study seeks to advance the incorporation of process-based predictions of surface-groundwater interactions to move toward efficient management of water resources.

2. STUDY SITES AND MODELING FRAMEWORK

2.1.Study sites description

We investigated the relative importance of base flow and seepage flow on the two Arguenon and Nançon headwater catchments located in the Brittany region (Fig. 1). Both catchments have been previously monitored for freshwater supply (Dewandel et al., 2021) and for water quality issues linked to high nitrate inputs for agriculture (Dupas et al., 2020; Widory et al., 2004). They are subject to the same temperate oceanic climate typical of the north-western regions of France. Hydrometeorological data, i.e. precipitation, evapotranspiration, infiltration and surface runoff - were extracted from the SAFRAN reanalysis and ISBA land surface model (Habets et al., 1999; Noilhan and Planton, 1989) available in the SURFEX modeling platform developed by the French meteorological service Météo-France on an 8 km by 8 km grid (Le Moigne, 2009; Masson et al., 2013). Climatic conditions are similar for both catchments with an average annual precipitation of about 850 mm/yr. On average 550 mm/yr returns to the atmosphere through evapotranspiration, 65 mm/yr runs off directly to the river network due to infiltration excess capacity and 235 mm/yr infiltrates and constitutes the aquifer recharge. Both catchments have similar morphologies with catchment areas of 104 km² and 67 km² for the Arguenon and Nançon, average slopes of 3-4% and divergent shapes, as typically encountered in Armorican landscapes (Crave and Davy, 1997; Lague et al., 2000). They differ by their drainage density with higher values for the Nançon (1.5 km^{-1}) compared to the Arguenon (0.67 km^{-1}) and by their average hillslope length of about 1000 m for the Nançon and about 2250 m for the Arguenon. The Arguenon also has less wetlands (5% of the surface compared to 9% for the Nançon) according to a field survey from the “water development and management plan” authorities.

Streamflow data are made available by the Regional Department for the Environment, Development and Housing (DREAL) at a daily time-step at the catchment outlets and are compiled in the national hydroportail database from 1970 to 2012 for the two catchments studied (http://www.hydro.eaufrance.fr/). Neither of the catchments is influenced by strong anthropogenic influences like dams or intensive pumping. Their annual water balances are similar as shown by their respective average specific discharge of 0.25 m/yr and 0.29 m/yr for the period 1970-2012. Their maximum peak specific discharges over the 42 years are of the order of 10^{-3} m/d. They differ by more pronounced low flows of 10^{-5} m/d for the Arguenon compared to 10^{-4} m/d for the Nançon. Such differences are classical in the Brittany region suggesting the potential influence of geological settings as previously suggested (Mougin et al., 2008). Both catchments are located in crystalline areas where the primary hydrodynamic properties coming from metamorphic and granitic rocks are known to be low (Gleeson et al., 2011b, 2014). They differ by their lithologies. The Nançon catchment is principally covered by granitic rocks, mainly granodiorite while the Arguenon is composed of around 25% of granitic rocks (granodiorite) and 75% of metamorphic rocks, mainly Brioverian schists and shales (Fig. 1). Secondary processes resulting from phases of erosion, tectonic activities and weathering have modified permeability and connectivity at the catchment scale (Ballèvre et al., 2009; Bonnet et al., 2000; Guillocheau et al., 2003), enhancing groundwater storage and flow as typically encountered in shallow subsurface aquifers (St. Clair et al., 2015; Taylor and Howard, 2000; Wyns et al., 2004). The structure of the aquifer system is described as stratiform composed from top to bottom of a capacitive saprolite layer, a transmissive fissured horizon and a poorly permeable fresh basement except for large tectonic fractures (Acworth, 1987; Dewandel et al., 2006; Roques et al., 2014, 2016; Taylor and Howard, 2000; Wright and Burgess, 1992).

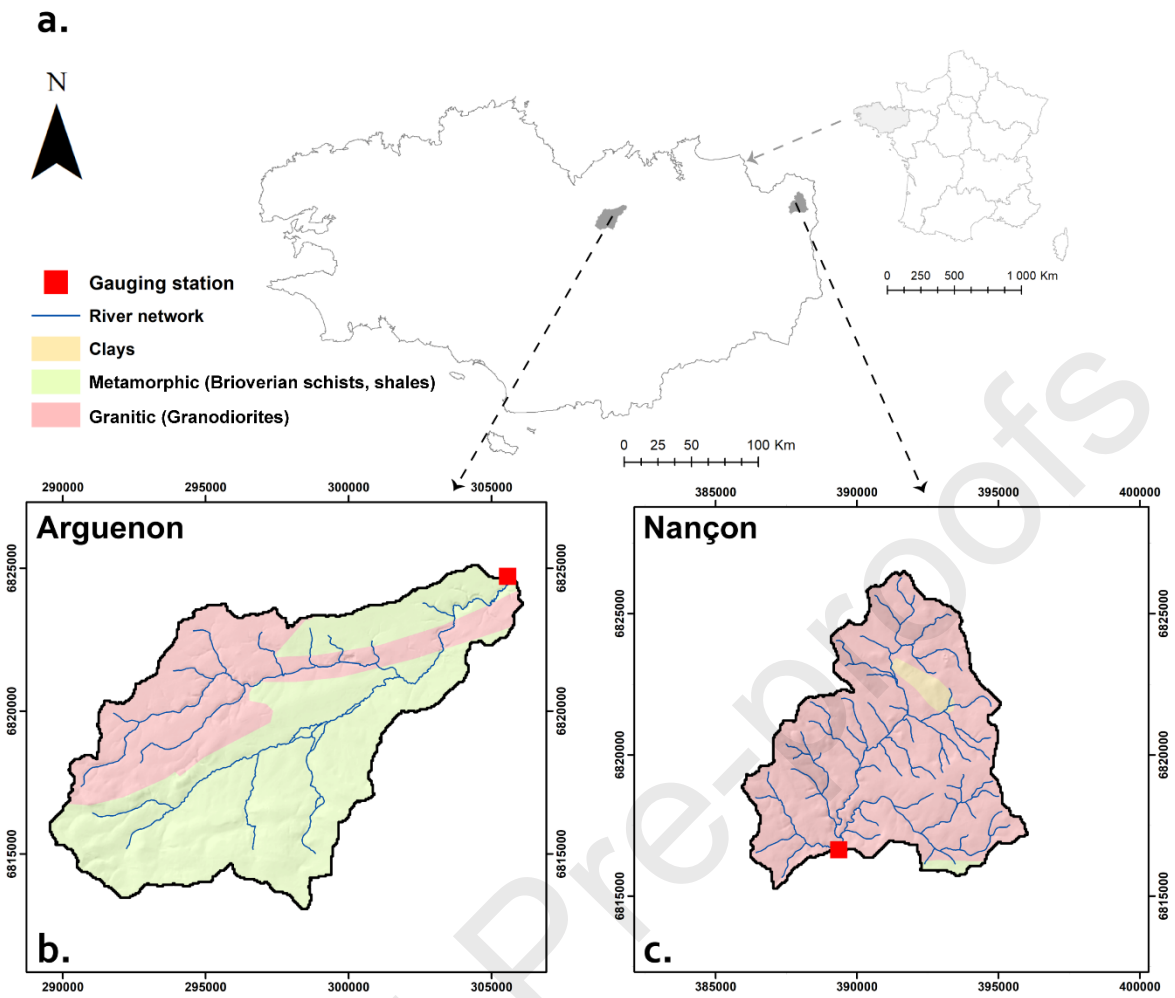

Fig. 1. Location and simplified geological map of the two headwater catchments Arguenon and Nançon. The red squares identify the locations of the gauging stations where discharge was measured.

2.2. Hydrological modeling scheme

2.2.1. Hydrometeorological model SURFEX

We use the land surface model SURFEX for the infiltration and surface runoff handled at a 8 km by 8 km resolution as forcing terms to the essential sub-grid hydrological processes modeled in this study (Fig. 2a) (Le Moigne et al., 2020; Masson et al., 2013; Vergnes et al., 2020a).

SURFEX is a modeling platform solving the water and energy budgets with the ISBA soil-biosphere-atmosphere model forced by the atmospheric inputs of the SAFRAN meteorological reanalysis (Durand et al., 1993; Quintana-Seguí et al., 2008; Vidal et al., 2010). SURFEX computes the partitioning of precipitations between evapotranspiration, surface runoff, and soil drainage considered as infiltration and thus as the aquifer recharge in this study (Decharme and Douville, 2006; Habets et al., 1999). The surface runoff is routed directly to the stream network through an offline coupling and added to the groundwater flows (Fig. 2b) computed from the implemented model (Caballero et al., 2007; Habets et al., 2008; Vergnes et al., 2020a). Note that we normalize the infiltration and surface runoff terms by the observed discharge to equilibrate the water balance (normalization factors of 1.24 for Arguenon and 0.94 for Nançon).

SAFRAN is an atmospheric analysis that was first devoted to the Alps mountain (Durand et al., 1993) and then extended to France (Quintana-Seguí et al., 2008) and is available for more than 60 years (Le Moigne et al., 2020; Vidal et al., 2010). SAFRAN associates in-situ data with atmospheric reanalysis to provide all the surface atmospheric variables (solid and liquid precipitations, 2m temperature and humidity, 10m wind speed, direct and diffuse solar radiation, atmospheric radiation). The ability of the SAFRAN analysis to reproduce the in-situ data was assessed (Quintana-Seguí et al., 2008; Vidal et al., 2010) with especially good results on temperature and precipitation, and outperforms other existing atmospheric analyses (Raimonet et al., 2017). The quality of the SAFRAN analysis was part of the choice of the Rhone basin for the GEWEW experiment devoted to aggregation (Boone et al., 2004). The land surface scheme Interactions between Soil, Biosphere, and Atmosphere model (ISBA) is devoted to estimate the surface fluxes for weather numerical model, and thus, a special attention was paid to the assessment of the evapotranspiration, using either direct in situ data (Decharme et al., 2019; Habets et al., 1999; Napoly et al., 2017) or water balance approaches (Boone et al.,

2004; Habets et al., 1999; Le Moigne et al., 2020). The ECOCLIMAP database provides physical parameters of the soil and vegetation at a resolution of 1 km by 1 km (Faroux et al., 2013; Masson et al., 2003).

In this study, the soil and vegetation parameters are averaged at the same scale than SAFRAN, so that a single estimation of the evapotranspiration is provided at that scale. However, it is known that some variations of the evapotranspiration flux can occur at finer spatial scale, due to land use contrast, especially hedgerow that used to be common in Brittany, and topography that affect soil moisture accumulation and connection with the groundwater (Thomas et al., 2012). It is a recurrent issue in hydrology that the characteristic scale of the climate forcings may be different from that of the processes and must involve sub-grid models. This is for example the case for mountain catchments where variations in topography on a scale of 100 meters must be taken into account to represent orographic effects, snow cover (Giorgi et al., 2003; Lafaysse et al., 2011), their consequences on the triggering of floods (Vincendon et al., 2010; Yu and Lane, 2011) and on the monitoring of groundwater resources (He et al., 2016; Henriksen et al., 2003; Vergnes et al., 2020b, 2014). Similarly, the hydrological dynamics of the Arguenon and Nançon requires the implementation of a sub-grid model that represents the saturation dynamics of the hillslope linked to the relative alternance between the base flow, seepage flow and overland flow, itself conditioned by the geomorphological and geological structures of the hillslope. This is precisely what we achieve in this study by combining the quality of SURFEX reanalyses for precipitation and evapotranspiration at the 8 km scale and the need to represent hillslope hydrological processes at a much finer scale to capture the distribution of fluxes between its different surface and subsurface components.

2.2.2. Hillslope morphology

The catchment area and stream network are defined from the location of the gauging station using the French Digital Elevation Model (DEM) BD ALTI® at a resolution of 25 m (https://geoservices.ign.fr/bdalti). We applied a surface flow accumulation routine to define the stream network and checked its accuracy with available 1:25000 maps from the national geographical institute (https://www.geoportail.gouv.fr). We assume that the hydrogeological catchment boundaries are similar to the one of the topographical one. This assumption is justified by the relatively low topographical gradients, the short hillslope lengths (1500 m) and the limited thickness of the aquifer on the order of 30 m (Gburek and Folmar, 1999; Kolbe et al., 2016; Roques et al., 2014).

From the DEM, we first compute the geometry of an equivalent hillslope at a resolution of 25 m for each of the catchments studied using standard DEM analysis methods (Bogaart and Troch, 2006; Schwanghart and Kuhn, 2010; Troch et al., 2003). The equivalent hillslope is defined by integrating the catchment properties on iso-distances to the streams. It is defined by its width profile $\omega(x)$ [m] and its topographical slope $\theta(x)$ [-] as functions of the iso-distance to the river x [m] (Fig. 2c,d) (Fan and Bras, 1998; Marçais et al., 2017). The equivalent hillslope is a simplified representation of the catchment integrating some of the main geomorphological characteristics of the catchment including the mean hillslope length, its planform shape (converging/diverging) and the overall evolution of its slope from the river to the water divide.

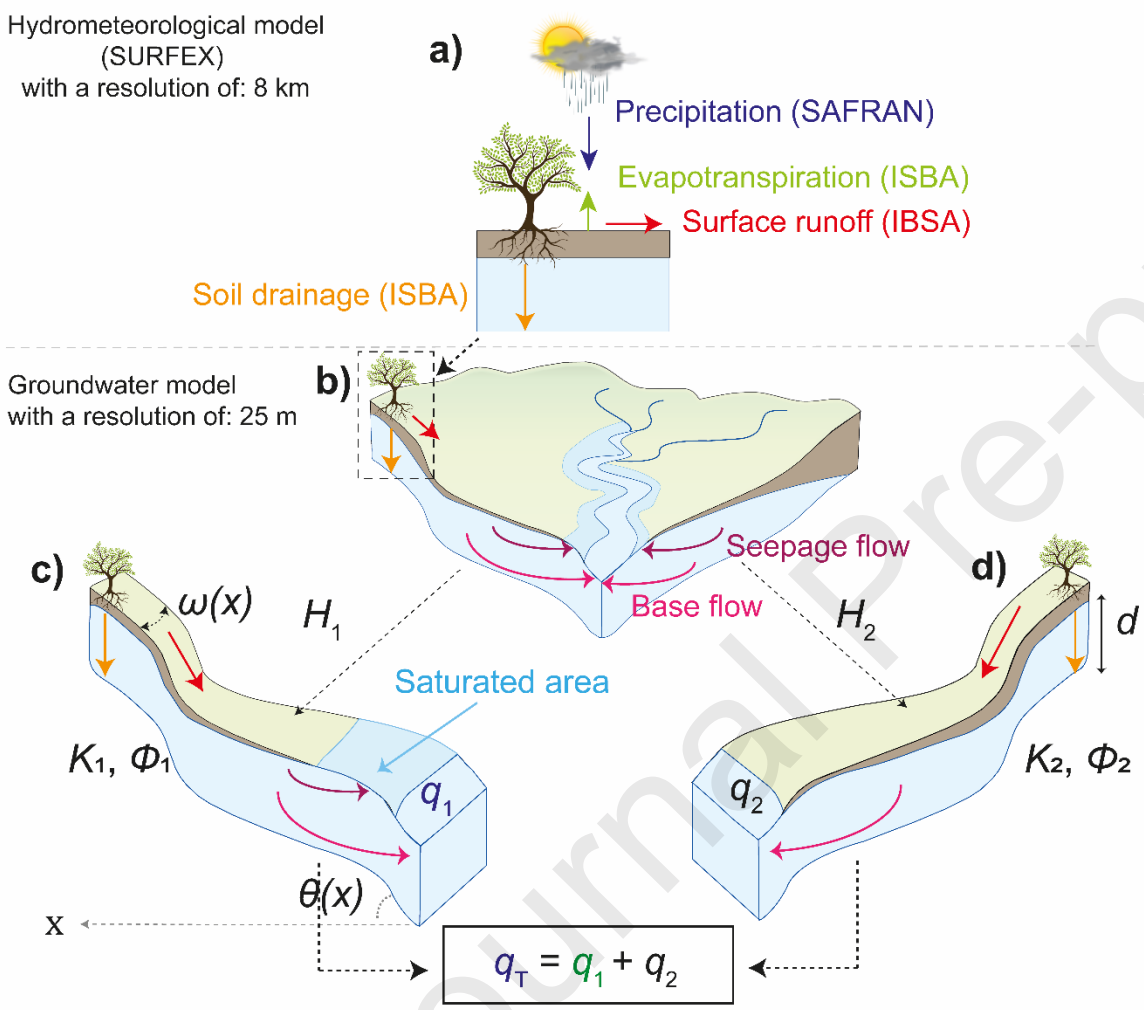

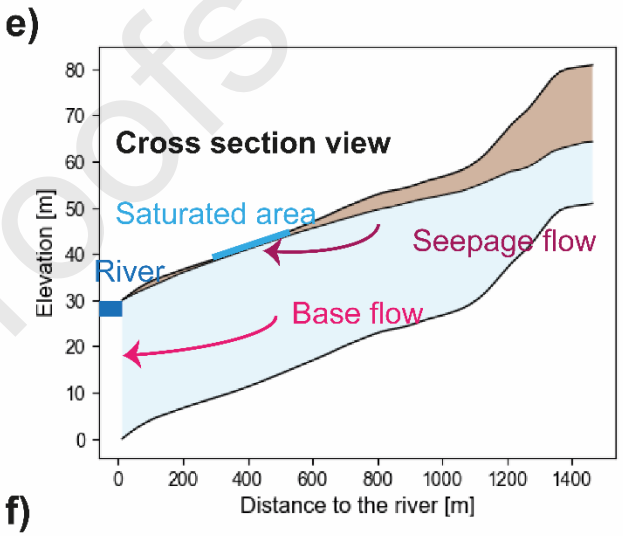

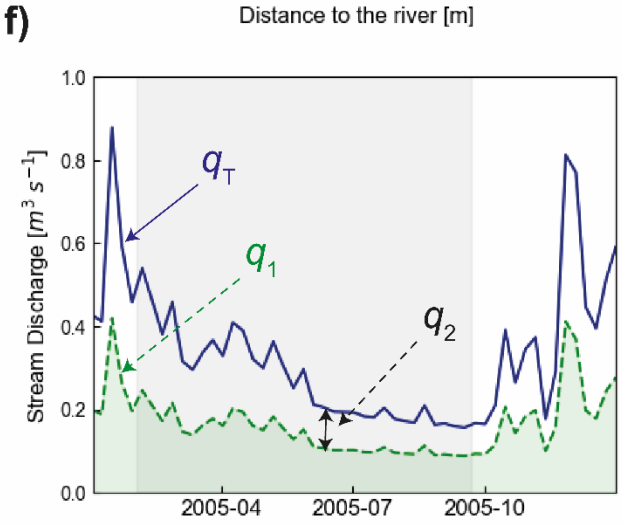

Fig. 2. Conceptual representation of the hydrological modeling scheme. a) The SURFEX hydrometeorological model partitions precipitation from SAFRAN reanalysis into surface runoff and infiltration at a resolution of 8 km. b) The groundwater model simulates the water table evolution and the hydrological sub-grid processes at a resolution of 25 m using the infiltration as input. When the water table reaches the surface, the generated seepage flow is added to the slow base flow and to the fast surface runoff routed directly to the river to yield the river discharge. c, d) The equivalent hillslope is duplicated in 2 equivalent hillslopes having the same morphology and hydroclimatic inputs but differing effective hydraulic properties to represent the spatial and temporal variations of the seepage flow and base flow. The two hillslopes sketch, respectively, a lower conductive hillslope H_1 (c) leading to a fast response with high seepage flows and a slow base flow (H_1 discharge q_1) and a higher conductive hillslope H_2 (d) with extended contribution after recharge periods (H_2 discharge q_2). e) Elevation profile of the equivalent hillslope as a function of the distance to the river at which processes are modeled. f) Hillslope contributions are summed to get the catchment scale discharge.

2.2.3. Equivalent hillslope Boussinesq model for groundwater flows

Base flow is modeled at the hillslope scale assuming that flows can be vertically integrated leading to the equation of Boussinesq (Boussinesq, 1877). It eventually relates the local discharge to the spatial and temporal change in storage (Hilberts et al., 2004; Paniconi et al., 2003; Troch et al., 2003). Interception of the water table with the surface is introduced by thresholding the storage capacity (Marçais et al., 2017). When the water table intersects the surface, the flow in excess is returned to the surface as seepage flow (Fig. 2e).

2.2.4. Effective parameterization

To represent the spatial variability in a parsimonious way, we duplicated the equivalent hillslope in two equivalent hillslopes H_1 and H_2. Both equivalent hillslopes have the same morphologic profiles and hydroclimatic inputs but different effective hydraulic conductivities K [m/s] and porosities ϕ [-] (Fig. 2c,d). Effective hydraulic properties are considered as a bulk representation of the distribution of hydraulic conductivity and porosity at the hillslope scale. It upscales the local heterogeneity arising from the presence of different lithologies, fractures, geological discontinuities and geometry of the weathering profile. We set a constant aquifer thickness d [m] of 30 m on both hillslopes in agreement with the observed thickness of shallow weathered/fractured compartment on the two pilot catchments (Mougin et al., 2008). This constant aquifer thickness is consistent with the general conceptual model of stratiform crystalline aquifers, whose thicknesses of the main transmissive aquifer are commonly estimated to be between 10 m and 40 m (Mougin et al., 2008). Hence the effective representation of the hillslope assumed a constant thickness of the conductive zone. Note that the 30 m thickness is larger by a factor of 10 than the annual water table fluctuation observed in the region (Dewandel et al., 2021; Kolbe et al., 2016; Mougin et al., 2008). Further results will be presented using the maximal water height defined as the product of the porosity with the aquifer thickness. We force the two equivalent hillslopes to contribute, on average, equally to the observed discharge by attributing the same representative area to each of them. Instantaneous contributions can still be highly different. We assumed that the surface runoff is uniformly distributed along the two equivalent hillslopes and add it to the hillslope flows Q_1 [m/d] and Q_2 [m/d] (Fig. 2f). Calibration of the groundwater model to the discharge data provides two sets of hydraulic conductivities and porosities.

2.3.Numerical methods

Uppermost and lowermost boundary conditions are taken as no-flows and fixed storage downstream to ensure a constant connection with the river. The resulting equations discretized with the mixed-element scheme leads to a differential-algebraic system of equations solved with the backward differentiation method implemented in the sundials software suite (Reynolds et al., 2019). All details can be found in Marçais et al. (2017).

In the relatively humid conditions considered in this study, the stream will be assumed to be always gaining and never losing. This agrees with local observations on the Nançon watershed made in summer 2017 (low water level conditions) by Dewandel et al. (2021) showing piezometric levels remaining above the stream elevation.

Effective hydraulic conductivities and porosities are calibrated by minimizing the error between observed and modeled discharge timeseries averaged at the weekly time scale. The weekly time scale has been chosen to highlight the processes related to the subsurface and filter the rapid processes occurring in the river. The approach is straightforwardly configured by the DEM analysis and enables a fast exploration of the parameter space for calibration, while also keeping a physical description of the base flow, of the seepage flow and of the variability of the saturated areas (Marçais et al., 2017). Calibration is performed by a regular logarithmic parameter space exploration from 10^{-8} to 10^{-2} m/s for the hydraulic conductivity based on previous studies on crystalline basement catchments in Brittany (Clément et al., 2003; Dewandel et al., 2021; Kolbe et al., 2016; Le Borgne et al., 2004; Martin et al., 2006; Roques et al., 2014). Porosity is explored in the range of 0.1% (Singhal and Gupta, 2010) to 50% (Kovács, 2011; Wright and Burgess, 1992). In the cases handled below, a resolution of 50 values for each of the parameters has been

found to be adequate. Finer resolutions tested on preliminary simulations led to the same conclusions.

Parameter space exploration has been optimized by performing the simulations first considering only one equivalent hillslope providing 2500 (50^2) aggregated simulations. Then, we aggregate again the simulations with their duplicates for the two-equivalent hillslope model, resulting in 6250000 (2500^2) simulations. Calibration is performed with two selection criteria described below:

- The first criterion refers to the presence of a saturated area developing uphill of the stream during the wet period as reported by previous works (Dewandel et al., 2021). Indeed, it is observed that, the relatively wet conditions of Brittany extend the saturated area to the side of the river during the recharge period. Assuming that the saturated area is not limited to the river is a critical point of the modeling approach to ensure representation of both seepage and base flows. Any model that would not comply with this criterion is excluded. It is especially the case of highly diffusive models for which the water table of the aquifer would remain all year much below the surface. Although defined as a binary selection criterion, i.e. of presence or absence of saturated area, we will see that it is a key constrain to reduce model uncertainty and describe the major processes involved.
- The second model selection criterion is related to the estimation of the catchment discharge. The Nash Sutcliffe Efficiency index (*Nash*) is taken as the optimization criterion (Nash and Sutcliffe, 1970). It is computed over the logarithm of the discharge data to equilibrate the relative importance of the low and high flows in the calibration process. Full agreement is obtained for a value of the *Nash-log* coefficient of 1. Models can be considered acceptable for Nash-log values larger than 0.65 and good when higher than 0.8 (Ritter and Muñoz-Carpena, 2013). Simulations were selected when their corresponding *Nash-log* value were

at least equal to 97.5% of the maximum *Nash-log* values obtained over the whole parameter exploration space.

3. RESULTS

3.1. Model performances

Models on both catchments were calibrated using the systematic exploration method described in section 2.3. Simulations were performed with the infiltration forcing term extracted from SURFEX (Fig. 3a,b). The calibrated models provide accurate representation of streamflow dynamics for both Arguenon and Nançon catchments (Fig. 3c,d). The modeled discharge (blue line) follows closely the observed discharge (red line) over the three year period displayed here (2004-2006) as well as for the full time series 1970-2012 (Figs. A.1-2-3). According to the two selection criteria given in section 2.3, 15845 and 10673 models out of the 6250000 models were retained. It represents around 0.2% of the total model explored with mean *Nash-log* values of 0.83 and 0.78 for the Arguenon and Nançon, respectively (Table 1). Despite their relatively large numbers, the calibrated models share the same trends as shown by their limited variability (cyan area on Fig. 3c,d).

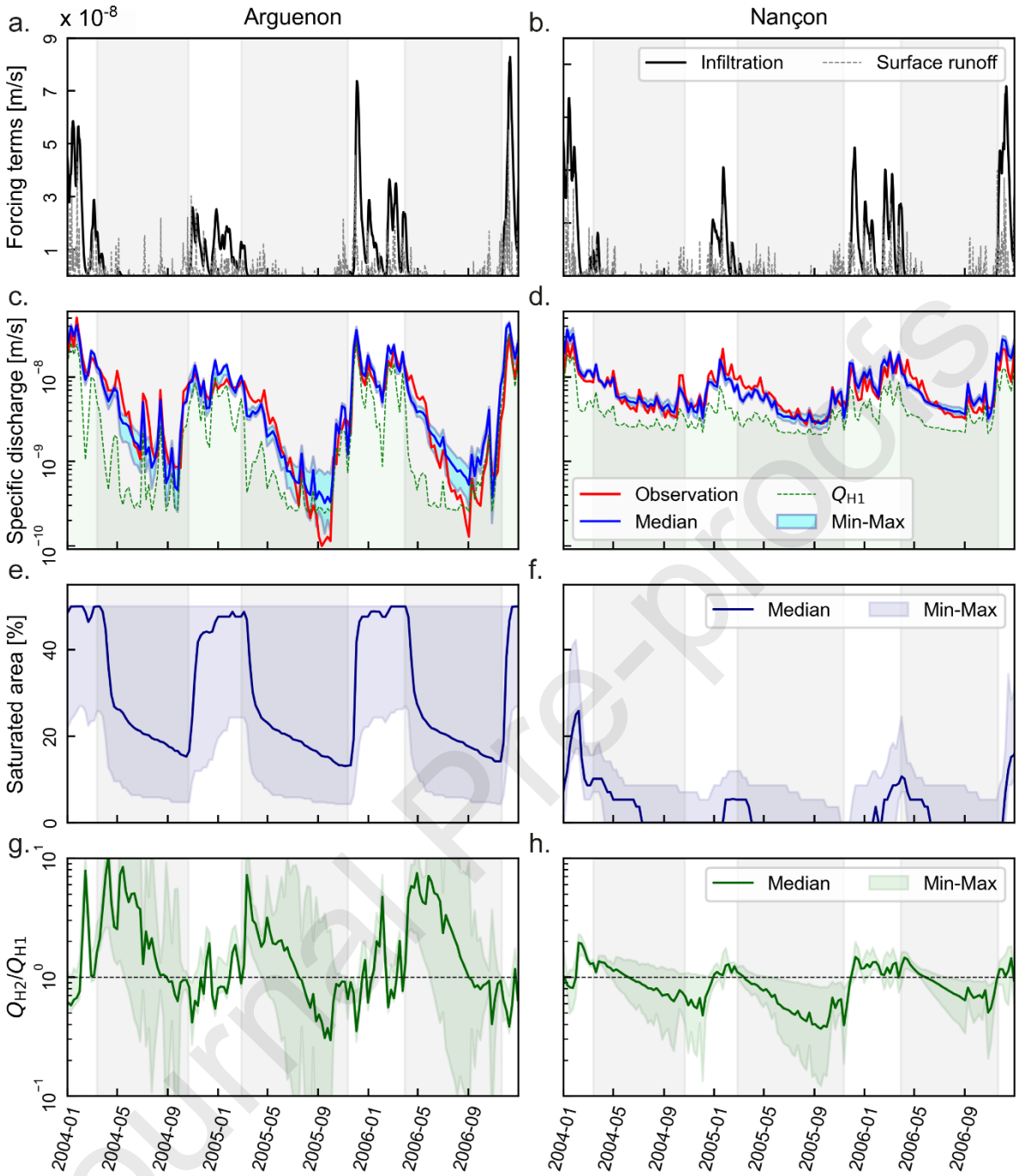

Fig. 3. Results and performances of the calibrated models for the 2004-2006 period. Results over the whole 1970-2012 period are given in Figs. A.1-2. Left and right columns represent respectively the results for the Arguenon and Nançon catchments. The successive grey and white bands underline the overall recession period from April to October and recharge period from November to March. a) and b) show the infiltration timeseries and the surface runoff given by the SURFEX hydrometeorological model. Precipitation and evapotranspiration timeseries are given in Appendix (Fig. A.4.) c) and d) display observed (red) and modeled (blue and green) specific discharge timeseries. Green curves represent the median discharge from the selected H_1 hillslope models, i.e. the hillslope with the lower hydraulic conductivity. The blue lines and cyan areas represent the cumulated modeled discharge and its variability for the two equivalent hillslopes H_1 and H_2. The difference between the blue and green curves illustrates the contribution of the less saturated hillslope H_2. e) and f) display the evolution of the median catchment saturated area among models (navy blue line) and its variability (navy blue area). g) and h) show the ratio of discharge between the two hillslopes Q_{H2}/Q_{H1}. The horizontal dashed line underlines the value of 1 above which discharge is dominantly controlled by the hillslope H_2 and below which it is dominated by H_1.

A detailed inspection of the discharge time series shows that the representation of both low and high flow dynamics are accurate without showing any systematic deviation. For the higher flows, the good model performances come from the quality of the reanalysis provided by the land-surface model SURFEX and by the ability of the groundwater model to partition the recharge flux to a part quickly routed to the river as seepage flow, and another part, much slower, transferred by base flow with a sub-grid discretization at a resolution of 25 m. The proportion of the discharge that is quickly routed to the river is conditioned by the extension of the saturated area. Larger saturated areas lead to more intense seepage flows during

precipitation events. It speeds up the response of the catchment and produces the rapid variations of the observed discharge. The modeled saturated area can go up to 50% of the total catchment surface for the Arguenon (Fig. 3e). It rapidly expands at the beginning of the wet season when the intensification of precipitations and the decrease of evapotranspiration enhance infiltration and groundwater storage. For the Nançon, the modeled saturated area displays lower values with less variability, in agreement with the high piezometric values only close to the streams (Fig. 3f). The limited extent of the modeled saturated area suggests higher infiltration rates and, in turn, higher transient storage with more resilient contribution to discharge during the recession period (Fig. 3d).

The higher buffering capacity of the Nançon is confirmed by the relative contributions of the two hillslopes H_1 and H_2 (Fig. 3e,f). For the Arguenon catchment, H_1 shows higher contributions to the total discharge during the high flow period (white bands) as shown by a predominance of Q_{H1} over Q_{H2} ($Q_{H2}/Q_{H1}<1$, Fig. 3g). An important proportion of the infiltration input is directly intercepted by the extended saturated area (Fig. 3e). Q_{H2}/Q_{H1} widely varies between 0.3 and 10. For the Nançon catchment, contributions of the two hillslopes appear to be more equilibrated with Q_{H2}/Q_{H1} only varying between 0.4 and 2 (Fig. 3h). The larger buffering capacities of the Nançon are directly related to smaller differences between the contributions of quick and slow hillslopes H_1 and H_2 and by lower heterogeneities as will be further investigated in the next section.

By the end of the recession, the contribution of H_1 becomes larger because H_2, with its higher diffusivity, emptied faster leading eventually to lower contributions. In some sense, the contributions of the two hillslopes tend to equilibrate in the low flow period when the less conductive hillslope compensates the lack of recharge by a slower discharge. Low flows thus appear to be a non-obvious combination of the contributions of the two hillslopes. It is not a

simple dominant contribution of one of the hillslopes nor a simple succession of contributions of the two hillslopes. It is a more intricate combination of the two hillslopes, the less diffusive hillslope catching up the more conductive one by the end of the low flow period. It also explains how the two-equivalent hillslope models can comply with a much larger diversity of low flow signals. It should eventually be noted that the combination of the hillslope contributions would be difficult to catch analytically as it does not only depend on their diffusivities but also on their initial storage, itself determined by the share between the recharge and the overland flow during the wet season.

3.2.Model parameters

Estimated hydraulic conductivities K_1 and K_2 from selected models cover five orders of magnitude between 2.8x10^{-8} m/s (Log K_1 = -7.56) and 2.8x10^{-3} m/s (Log K_2 = -2.55) (Table 1). They span the full range of values explored by the model (set to 10^{-8}-10^{-2} m/s). For both Arguenon and Nançon, the two hillslopes H_1 and H_2 display quite different properties. The hydraulic conductivity and maximal water height of H_1 are better defined than the ones of H_2. K_1 and $\phi_1 d$ vary by factors of 21 and 11, respectively, while K_2 and $\phi_2 d$ range by factors of 100 and 50. K_2 and $\phi_2 d$ are poorly defined but the diffusivity $K_2 d/\phi_2$ is well constrained and only ranges by a factor of 4 at most. The less pervious hillslope (H_1) has a well-defined hydraulic conductivity while the more pervious hillslope (H_2) is characterized by a well-defined diffusivity. We investigate more closely the specific hydraulic behaviors of H_1 and H_2.

Table 1. Calibrated parameters and model performance

	Arguenon			**Nançon**		
	min	***mean***	***max***	***min***	***mean***	***max***
Log K_1	-7.56	-6.89	-6.23	-5.72	-5.66	-5.62
***ϕ_1 d* [m]**	1.3	3.7	8.9	1.3	6.8	15.0
Log K_2	-4.29	-2.80	-2.55	-5.21	-3.98	-3.37
***ϕ_2 d* [m]**	0.3	6.8	15.0	0.6	7.8	15.0
Log K_1 d/ϕ_1	-5.5	-4.32	-3.37	-3.94	-3.42	-2.76
Log K_2 d/ϕ_2	-0.86	-0.67	-0.44	-2.25	-1.92	-1.59
Log K_2/K_1	2.24	4.28	5.0	0.41	1.68	2.24

We identify the hydraulic behaviors of H_1 and H_2 considering the mean saturated area. Fig. 4 shows phase diagrams of the hydraulic conductivity K on the x-axis along with the maximum water height $\phi\, d$ on the y-axis. Blue and red dots identify the calibrated hydraulic parameters of H_1 and H_2, respectively. The mean saturated area is represented by the background color map. Fig. 4 shows the restricted range of hydraulic conductivities K_1 and the broader range of maximum water height $\phi_1\, d$. K_1 sets the location of the water table for an average steady state recharge. K_1 thus primarily determines the proximity of the aquifer to the surface and its ability to overflow along the hillslope as seepage flow. By comparison, $\phi_1\, d$ only modulates the temporal variations of the storage and saturated area (Fig. 4a). For the Nançon, the mean saturated area in fact does not depend on the maximal water height. It only evolves with the hydraulic conductivity and remains limited to a range of 5% to 20% (Fig. 4b). As no constraint was given a priori on the range of saturated area beyond the requirement of its existence, the correlation between the calibrated hydraulic conductivity and the intermediary saturation values is a genuine property of the model in cases where overland flows remain limited like for the Nançon. For the more variable overland flows displayed by the Arguenon catchment, the porosity ϕ_1 also intervenes through its influence on the range of variations of the hydraulic head

and of the relative extension of the saturated area between the wetter and dryer seasons (Fig. 4a). For both catchments, the hydraulic behavior of H_1 adds up the two processes of a continuous base flow limited by a small conductivity and an intermittent seepage flow dominantly determined by the hydraulic conductivity and secondarily influenced by the porosity. The hillslope H_2 has a simpler behavior without any saturated area and thus with base flow as the only transfer process confirming the previously discussed control by the diffusivity $K_2 d/\phi_2$.

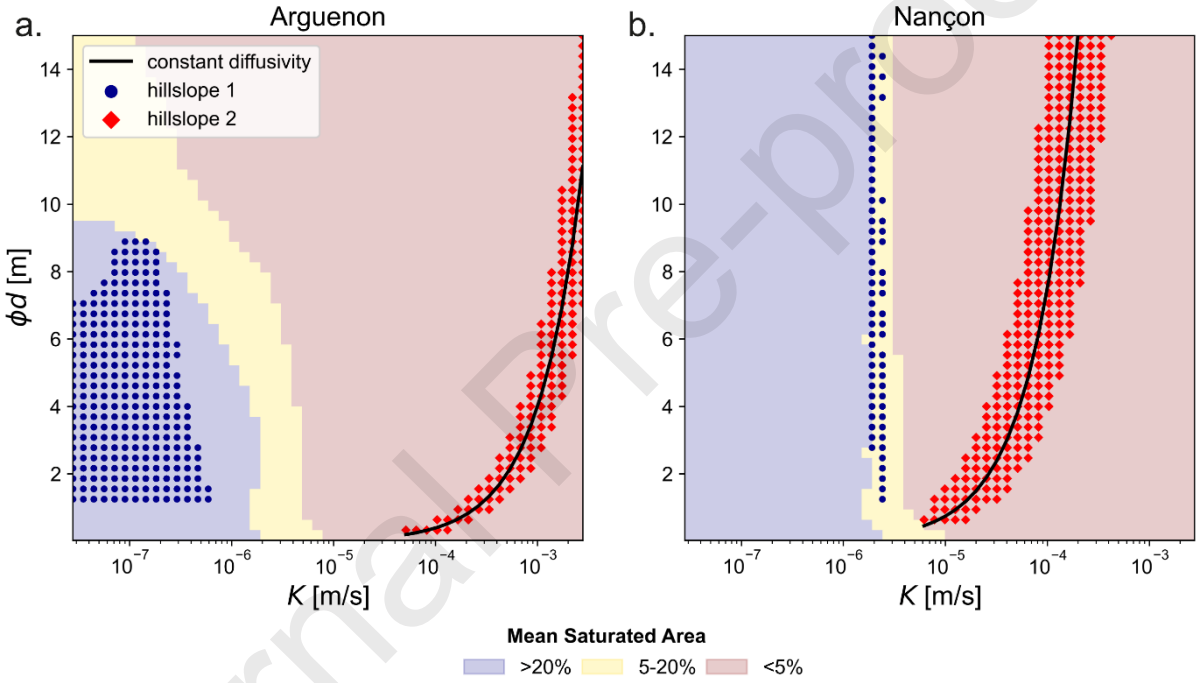

Fig. 4. Calibrated parameters of H_1 and H_2 marked by the blue and red dots respectively on top of the mean percentage of saturated area for a single hillslope (colormap) for the Arguenon (a) and Nançon (b). The black curve represents the mean constant diffusivity of the calibrated H_2 models (Table 1).

The contrast of hydraulic conductivities K_2/K_1 between the two hillslopes ranges between 0.4 and 2.2 orders of magnitude for the Nançon and between 2.2 and 5 orders of magnitude for the

Arguenon (*Table 1, Fig. A.5*). Even the smallest ratios remain significantly larger than 1 (around 3 and 100, respectively) showing that models with a single effective hillslope would result in larger discrepancies to the observed discharge. This is confirmed by the comparison of the seasonal variations of discharge obtained for the calibrated two-hillslope models and the best single hillslope model (Fig. 5). The single-hillslope model fails to capture both the amplitude and the temporality of the discharge data. Even more critically, the seasonal low flows are systematically overestimated by a factor of 2 for the Arguenon and by 30% for the Nançon. This would lead to significant bias in the assessment of the resources under current climates and, likely even more, under future climates. Heterogeneity in the catchment represented by the difference of the two hillslopes thus appears to be not only sufficient but also necessary to recover the main characteristics of the discharge data.

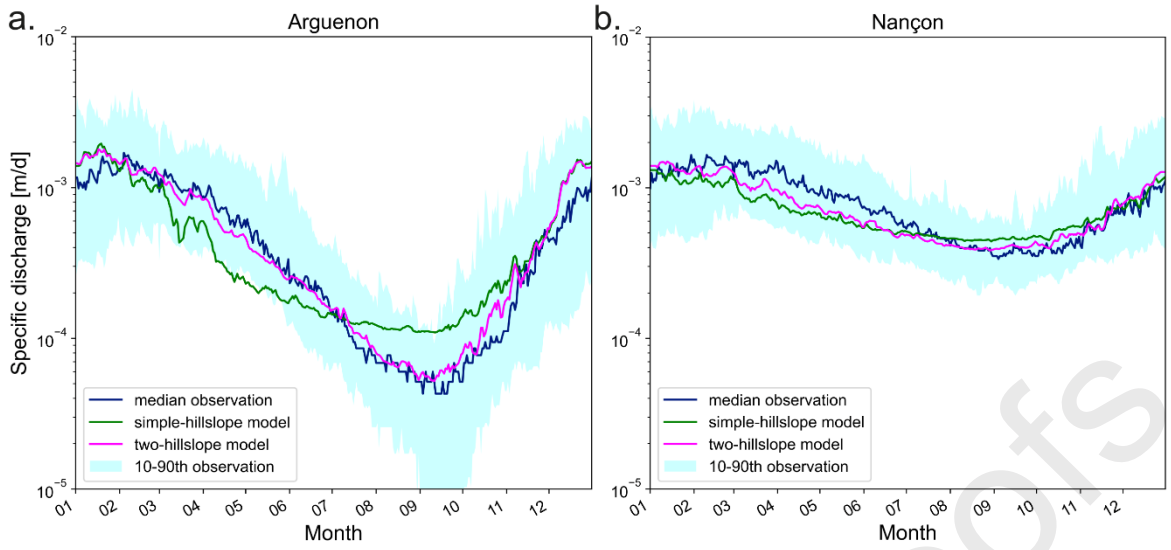

Fig. 5. Seasonal variations of specific discharge obtained by taking the mean over the 1970-2012 period for the median two-hillslope and best single-hillslope models for the Arguenon (a) and Nançon (b). Blue curve and cyan areas represent the median and the 10-90th quantile of observed discharge.

4. DISCUSSION

The transfer of water at the catchment scale is driven by processes operating at variable spatial and temporal scales. Such variability is highly dependent on the interaction between the base flow, the development of a saturated area at the surface and the intermittency of seepage flow. Our model calibration performed on observed discharge time series has shown that sharp contrasts in hydraulic conductivities between the two equivalent hillslopes (H_1 and H_2) were required to ensure accurate predictions over the full spectrum of timescales, with at least a factor of 3, and, on average, 3 orders of magnitude, between K_1 and K_2. We successively discuss:1) the consistency of these results with the available geological and hydrological information; 2) the emerging characteristics of the observed and modeled hydrological behaviors; 3) the

consequences on the interpretation of discharge data; and 4) the perspectives for the characterization and modeling of groundwater – surface water interactions in shallow aquifers.

4.1. Results consistency with the available geological and hydrological information

The degree of hydraulic heterogeneity emerging from the model is consistent with the differences in lithological units present in the catchment (Fig. 1). The hydraulic conductivities ratios inferred for the Arguenon catchment are by far larger than for the Nançon (Table 1, Fig. A.5). The Arguenon appears to be more heterogeneous than the Nançon. It is consistent with the geological map (Fig. 1). The Arguenon is characterized by a more heterogeneous geology, with the presence of two distinct lithologies, i.e., Brioverian schists (and shales) and granodiorite covering, respectively, 70% and 30% of the drainage area. The Nançon has mostly a homogeneous lithology, with the dominance of granodiorites.

A detailed analysis of the calibrated parameters shows that the maximum values of hydraulic conductivities K_1 stand in close range for both catchments, which might be characteristic of the common granodiorite lithology. The estimated hydraulic conductivities are effective properties of the hillslopes. They upscale the lithology and the local heterogeneities arising from fractures, weathering and erosion structures. For the Nançon, the values of K_1 (1.9×10^{-6} m/s to 2.4×10^{-6} m/s) are consistent with estimates from a well test analysis (mean $K = 5.5 \times 10^{-6}$ m/s) and piezometric inversion (mean $K = 3.9 \times 10^{-6}$ m/s) performed on the same catchment in (Dewandel et al., 2021). These values also agree with estimates from well tests in other granitoid formations of the Armorican massif (Clément et al., 2003; Le Borgne et al., 2004; Martin et al., 2006; Mougin et al., 2008, 2016). For the Arguenon, the lowest values of K_1 might be linked to the properties of the metamorphic lithology (Brioverian schists and shales). We

hypothesize that such characteristics arise from differences in mechanical and rock texture properties, providing higher potential for fracturing and weathering to granites and enhancing their bulk permeability (Riebe et al., 2017; Worthington et al., 2016).

Overall, these results suggest that lithological information might be at least partially correlated with the estimated effective hydraulic properties. Previous studies have explored the control of geology on hydrological behaviors, revealing strong differences among classes of lithologies categorized as crystalline, carbonates, fine and coarse sedimentary rock (e.g. Carlier et al., 2018; Floriancic et al., 2022; Gleeson et al., 2011b). In the present case, the region is mostly composed of crystalline aquifer with only a few percent of the area covered by sedimentary aquifers. The correlation between lithology and effective hydraulic properties might however be only partial, since permeability may be enhanced by secondary fracturing, weathering and erosion processes, which are highly variable across bedrock regions because of tectonic, paleoclimate and geomorphological evolutions (Acworth, 1987; Boutt et al., 2010; Dewandel et al., 2006; Krasny, 2002; Lachassagne et al., 2021; Riebe et al., 2017; Wyns et al., 2004). Aquifers in crystalline rocks are characterized by strong spatial and vertical heterogeneities even within a single lithology (Courtois et al., 2010; Dewandel et al., 2021; Gleeson et al., 2009; Lachassagne et al., 2021; Le Borgne et al., 2004). Such heterogeneities often limit simple upscaling of locally determined hydrodynamic parameters through well tests (Clauser, 1992) and motivate the development and deployment of larger scale assessment of effective hydraulic properties. At the catchment scale, while weathering profiles may be visible in some parts, it can as well be removed by erosion. In that case, the transfer of water would be controlled by the underlying fractured bedrock resulting in different dynamic and hydrological behaviors (Dewandel et al., 2021; Kolbe et al., 2016; Mougin et al., 2008). As shown by the quality of the model results at the hillslope scale, effective parameters integrating those local heterogeneities

can effectively represent the observed hydraulic behaviour. Similar conclusions have been drawn from other studies and geological settings. In sandy and clayey loams, hydraulic properties evaluated from stream discharge time series lead to heterogeneous estimates for close lithologies (Matonse and Kroll, 2009). Regional scale analyses should be performed to confirm the informational content of the geological map on the hillslope- to catchment-scales hydrogeological characteristics.

4.2. Emerging diversity of hydrological behaviors

From the analysis of the hydrographs, both catchments display highly differing hydrological behaviors. Our modeling approach enables us to describe the relative importance of:1) base flow; 2) saturated area development; and 3) seepage flow in controlling this difference.

1) In the case of the Arguenon, the catchment responds with high variability in specific discharge spanning over more than 2 orders of magnitude. High flows are well predicted by rapid transfers over the persistent saturated area of H_1 as seepage flow. The falling limb of the hydrograph after the recharge season is well captured by the second hillslope H_2. Its high diffusivity ensures the observed rapid drainage of the aquifer. At the end of the wet season, the hillslope H_1 has been marginally recharged and the hillslope H_2 is quickly discharging. Consequently, groundwater discharge to the river decreases sharply and remains limited to the small contribution of H_1, suggesting a low resilience of the groundwater resource.

2) In the case of the Nançon, the specific discharge is less variable, ranging over less than an order of magnitude between the recharge and recession seasons (Fig. 5). In the recession period, streamflow is supported by the contributions of both H_1 and H_2 reaching typically 2/3 and 1/3 of the discharge (Fig. 3h). The low variability and streamflow dynamics of the recession periods both suggest a more resilient groundwater discharge over a long drainage period.

The difference in hydrological behavior between the two catchments shows the role of groundwater-surface water interactions and their characteristic times in shaping the catchment-scale storage-discharge responses. It confirms the significant variety of hydrological responses across catchment lithology and heterogeneity discussed by the critical zone community (Blöschl et al., 2019; Fan, 2015; Gauthier et al., 2009; Gleeson et al., 2009; Harman et al., 2009; Hartmann, 2016; Hartmann et al., 2017).

4.3. Consequences on the interpretation of discharge data

The combination of hydrological processes operating at various timescales conditions the interpretation of discharge hydrographs. The analysis of streamflow recessions during low flow periods is the classical methodology used to evaluate catchment to regional scale hydraulic properties (Brutsaert and Lopez, 1998; Brutsaert and Nieber, 1977; Mendoza et al., 2003; Parlange et al., 2001; Troch et al., 1993; Vannier et al., 2014; Wittenberg, 1999). It assumes a simple linear or power law relationship between the discharge and its derivative over time. It assesses the non-linearity in storage-discharge functions (Berghuijs et al., 2016; Kirchner, 2009; Tashie et al., 2020a), and the resilience of water resources to climate change (Jachens et al., 2020; Tashie et al., 2019, 2020b). It relies on the prediction of the rate of change in stream discharge as a function of the reduction of head, storage and, consequently, flow from the aquifer connected to the stream (for a review, see Troch et al., 2013).

In cases where the aquifer water table remains under close interaction with the surface, such as those investigated here, the time periods over which this condition is fulfilled are difficult to identify. For extended periods, the catchment response is a function of the groundwater system but also from the late prevalence of the saturated area (Fig. 3e,f). It reduces the duration of the exploitable discharge and limits the capacity to identify long response times. More

fundamentally, short and long response times resulting from the hydraulic heterogeneity might both intervene on related periods of time and be difficult to identify independently. It would help explain the observed range of recession timescales often reported in discharge interpretations (Harman et al., 2009; Jachens et al., 2020; Tashie et al., 2020a). By filtering the short response times, the proposed methodology provides accurate predictions for the long response times making up the main recession signal previously shown by Fig. 5. This prediction is essential for the evaluation of the resilience of water resources through classical statistical metrics like the 5 Years Mean Monthly Annual Minimum discharges (*5MMAM*) or the 7-days low flow's (*7Q2*; *7Q10*) commonly used for water resources management in the drier season (Fangmann and Haberlandt, 2019; Van Loon and Laaha, 2015).

4.4. Perspectives for the characterization and modeling of groundwater – surface water interactions in shallow aquifers

Mechanistic approaches for resolving subsurface flows and their interactions with the surface are important to assess the vulnerability of water resources to climate change. Among increasingly available physically based integrated surface-subsurface models (Aquanty, 2016; Kollet and Maxwell, 2006; Paniconi and Putti, 2015; Sulis et al., 2010), the hillslope approach used here presents the capacity to account in an effective way for both the groundwater dynamics and their interception with the surface (Marçais et al., 2017). Like other mechanistic approaches, it separates the geological influences from the climatic influences in these conditions where the proximity of the aquifer to the surface can rapidly develop saturated area or where evaporation might be enhanced by abundant shallow subsurface water (Maxwell and Kollet, 2008). The interest of the mechanistic models is reinforced by the numerous studies that have highlighted the role of saturated areas on the hydrological behavior and especially on the recession period (Ambroise, 2016; Lana-Renault et al., 2014).

Mechanistic models require additional observations for their calibration at a regional scale. While data of hydraulic head variations are interesting, providing direct information on the aquifer location and dynamics, they are also highly sensitive to local heterogeneities, preventing their use at regional scale. Saturated areas might be more generally available at a regional scale. The rate of change in saturated area is more difficult to determine. It results both from natural and anthropic factors. On some Britain catchments, the saturated area has been reduced by the intensive agricultural drainage developed. The observed saturated area would thus be likely smaller than expected. Saturated area would require additional analysis to be interpreted not so much in terms of overall quantity, which might be biased, but more in terms of location within the catchment and any information relating the groundwater interactions of the saturated areas with the river network (Antonelli et al., 2020; Glaser et al., 2018, 2020).

5. CONCLUSION

We analyzed the hydrological response of two catchments of 67 km^2 and 104 km^2 using discharge data over 40 years. The temperate climate, low relief and crystalline basement favor shallow subsurface transfers and close interactions with the surface. We use a parsimonious hillslopes-scale model to investigate the spatial and temporal variability of the catchment response. We find that, for both sites, the catchment response cannot be interpreted by a single equivalent hillslope but require two equivalent hillslopes of different hydraulic properties. One of the hillslopes is characterized by a low hydraulic conductivity between $2.8x10^{-8}$ m/s and $2.4x10^{-6}$ m/s. The aquifer remains close to the surface and the water table intersects the surface in the wetter season. The saturated area recedes slowly after the main recharge period. It provides rapid saturation-excess and infiltration-excess overland flows on the surface as well as slow subsurface transfers. The other hillslope has large diffusivities between $5.6x10^{-3}$ m^2/s and $3.6x10^{-1}$ m^2/s. It provides intermediary response times supporting the stream discharge at

the beginning of the dryer season. Low flows are supported by a complex combination of both hillslopes depending both on their response time and on their amount of recharge in the previous wetter season. The two sites display qualitatively similar behaviors. They differ by their degree of hydraulic heterogeneities, and, in turn, by the variability of their discharge and their resilience to extended dry periods. Our results show that catchment responses involve temporally and spatially varying transfer processes well captured by parsimonious mechanistic approaches based on hillslope-scale processes. They also show that hydraulic properties remain heterogeneous at the catchment scale. Conversely, they suggest that catchment-scale hydrological responses might be used to characterize effective hydrogeological properties in regions dominated by shallow subsurface transfers. They motivate more extensive regional approaches to map hydrogeological properties of crystalline basements from a correlative analysis of discharge data and geological information. They eventually contribute to the representation of the water cycle at the hillslope scale taken as sub-grid processes of the global climate models, which give the major trends of atmospheric and surface processes but cannot go down to the more local hillslope scales.

Acknowledgments

The BRGM and Regional Council of Brittany are acknowledged for their funding support. Clément Roques acknowledges funding from the Rennes Métropole research chair “Ressource en Eau du Futur” and the European project WATERLINE, project id CHIST-ERA-19-CES-006. The authors also thank members of the Creseb working group on water and climate change for their support to the project and their input to the discussions. This working group includes drinking water operators and catchment managers (SDAEP22, SMG35, Eau du Morbihan, les SAGE de l'Arguenon-Baie de la Fresnaye et du Couesnon). We thank reviewers for their fruitful suggestions improving the quality of the paper.

References

Abbott, B.W., Bishop, K., Zarnetske, J.P., Minaudo, C., Chapin, F.S., Krause, S., Hannah, D.M., Conner, L., Ellison, D., Godsey, et al., 2019. Human domination of the global water cycle absent from depictions and perceptions. Nat. Geosci. 12, 533–540. https://doi.org/10.1038/s41561-019-0374-y

Acworth, R.I., 1987. The development of crystalline basement aquifers in a tropical environment. Q. J. Eng. Geol. Hydrogeol. 20, 265–272. https://doi.org/10.1144/GSL.QJEG.1987.020.04.02

Ala-aho, P., Soulsby, C., Wang, H., Tetzlaff, D., 2017. Integrated surface-subsurface model to investigate the role of groundwater in headwater catchment runoff generation: A minimalist approach to parameterisation. J. Hydrol. 547, 664–677. https://doi.org/10.1016/j.jhydrol.2017.02.023

Ambroise, B., 2016. Variable water-saturated areas and streamflow generation in the small Ringelbach catchment (Vosges Mountains, France): the master recession curve as an equilibrium curve for interactions between atmosphere, surface and ground waters. Hydrol. Process. 30, 3560–3577. https://doi.org/10.1002/hyp.10947

Anderson, M.G., Burt, T.P., 1978. The role of topography in controlling throughflow generation. Earth Surf. Process. 3, 331–344. https://doi.org/10.1002/esp.3290030402

Antonelli, M., Glaser, B., Teuling, A.J., Klaus, J., Pfister, L., 2020. Saturated areas through the lens: 2. Spatio-temporal variability of streamflow generation and its relationship with surface saturation. Hydrol. Process. 34, 1333–1349. https://doi.org/10.1002/hyp.13607

Aquanty, 2016. HydroGeoSphere user manual. Release 1.0. Aquanty Inc, Waterloo, Ontario, Canada.

Aryal, S.K., Mein, R.G., O'Loughlin, E.M., 2003. The concept of effective length in hillslopes: assessing the influence of climate and topography on the contributing areas of catchments. Hydrol. Process. 17, 131–151. https://doi.org/10.1002/hyp.1137

Aryal, S.K., O'Loughlin, E.M., Mein, R.G., 2002. A similarity approach to predict landscape saturation in catchments. Water Resour. Res. 38, 1208. https://doi.org/10.1029/2001WR000864

Ballèvre, M., Bosse, V., Ducassou, C., Pitra, P., 2009. Palaeozoic history of the Armorican Massif: Models for the tectonic evolution of the suture zones. Comptes Rendus Geosci., Mécanique de l'orogénie varisque : Une vision moderne de le recherche dans le domaine de l'orogénie 341, 174–201. https://doi.org/10.1016/j.crte.2008.11.009

Bartsch, S., Frei, S., Ruidisch, M., Shope, C.L., Peiffer, S., Kim, B., Fleckenstein, J.H., 2014. River-aquifer exchange fluxes under monsoonal climate conditions. J. Hydrol. 509, 601–614. https://doi.org/10.1016/j.jhydrol.2013.12.005

Berghuijs, W.R., Hartmann, A., Woods, R.A., 2016. Streamflow sensitivity to water storage changes across Europe. Geophys. Res. Lett. 43, 1980–1987. https://doi.org/10.1002/2016GL067927

Blöschl, G., Bierkens, M.F.P., Chambel, A., Cudennec, C., Destouni, G., Fiori, A., Kirchner, J.W., McDonnell, J.J., Savenije, H.H.G., Sivapalan, M., et al., 2019. Twenty-three unsolved problems in hydrology (UPH) – a community perspective. Hydrol. Sci. J. 64, 1141–1158. https://doi.org/10.1080/02626667.2019.1620507

Bogaart, P.W., Troch, P.A., 2006. Curvature distribution within hillslopes and catchments and its effect on the hydrological response. Hydrol. Earth Syst. Sci. 10, 925–936. https://doi.org/10.5194/hess-10-925-2006

Bonnet, S., Guillocheau, F., Brun, J.-P., Van Den Driessche, J., 2000. Large-scale relief development related to Quaternary tectonic uplift of a Proterozoic-Paleozoic basement: The Armorican Massif, NW France. J. Geophys. Res. Solid Earth 105, 19273–19288. https://doi.org/10.1029/2000JB900142

Boone, A., Habets, F., Noilhan, J., Clark, D., Dirmeyer, P., Fox, S., Gusev, Y., Haddeland, I., Koster, R., Lohmann, D., et al., 2004. The Rhône-Aggregation Land Surface Scheme Intercomparison Project: An Overview. J. Clim. 17, 187–208. https://doi.org/10.1175/1520-0442(2004)017<0187:TRLSSI>2.0.CO;2

Boussinesq, J., 1877. Essai sur la théorie des eaux courantes. Impr. nationale.

Boutt, D.F., Diggins, P., Mabee, S., 2010. A field study (Massachusetts, USA) of the factors controlling the depth of groundwater flow systems in crystalline fractured-rock terrain. Hydrogeol. J. 18, 1839–1854. https://doi.org/10.1007/s10040-010-0640-y

Bresciani, E., Davy, P., de Dreuzy, J.-R., 2014. Is the Dupuit assumption suitable for predicting the groundwater seepage area in hillslopes? Water Resour. Res. 50, 2394–2406. https://doi.org/10.1002/2013WR014284

Brutsaert, W., 2005. Hydrology: An Introduction. Cambridge University Press.

Brutsaert, W., Lopez, J.P., 1998. Basin-scale geohydrologic drought flow features of riparian aquifers in the Southern Great Plains. Water Resour. Res. 34, 233–240. https://doi.org/10.1029/97WR03068

Brutsaert, W., Nieber, J.L., 1977. Regionalized drought flow hydrographs from a mature glaciated plateau. Water Resour. Res. 13, 637–643. https://doi.org/10.1029/WR013i003p00637

Caballero, Y., Voirin-Morel, S., Habets, F., Noilhan, J., Le Moigne, P., Lehenaff, A., Boone, A., 2007. Hydrological sensitivity of the Adour-Garonne river basin to climate change. Water Resour. Res. 43, W07448. https://doi.org/10.1029/2005WR004192

Carlier, C., Wirth, S.B., Cochand, F., Hunkeler, D., Brunner, P., 2018. Geology controls streamflow dynamics. J. Hydrol. 566, 756–769. https://doi.org/10.1016/j.jhydrol.2018.08.069

Chae, G.-T., Yun, S.-T., Kim, K., Mayer, B., 2006. Hydrogeochemistry of sodium-bicarbonate type bedrock groundwater in the Pocheon spa area, South Korea: water–rock interaction and hydrologic mixing. J. Hydrol. 321, 326–343. https://doi.org/10.1016/j.jhydrol.2005.08.006

Clauser, C., 1992. Permeability of crystalline rocks. Eos Trans. Am. Geophys. Union 73, 233–238. https://doi.org/10.1029/91EO00190

Clément, J.-C., Aquilina, L., Bour, O., Plaine, K., Burt, T.P., Pinay, G., 2003. Hydrological flowpaths and nitrate removal rates within a riparian floodplain along a fourth-order stream in Brittany (France). Hydrol. Process. 17, 1177–1195. https://doi.org/10.1002/hyp.1192

Condon, L.E., Maxwell, R.M., 2015. Evaluating the relationship between topography and groundwater using outputs from a continental-scale integrated hydrology model. Water Resour. Res. 51, 6602–6621. https://doi.org/10.1002/2014WR016774

Courtois, N., Lachassagne, P., Wyns, R., Blanchin, R., Bougaïré, F.D., Somé, S., Tapsoba, A., 2010. Large-Scale Mapping of Hard-Rock Aquifer Properties Applied to Burkina Faso. Groundwater 48, 269–283. https://doi.org/10.1111/j.1745-6584.2009.00620.x

Crave, A., Davy, P., 1997. Scaling relationships of channel networks at large scales: Examples from two large-magnitude watersheds in Brittany, France. Tectonophysics 269, 91–111. https://doi.org/10.1016/S0040-1951(96)00142-4

Dahl, M., Nilsson, B., Langhoff, J.H., Refsgaard, J.C., 2007. Review of classification systems and new multi-scale typology of groundwater–surface water interaction. J. Hydrol. 344, 1–16. https://doi.org/10.1016/j.jhydrol.2007.06.027

Decharme, B., Delire, C., Minvielle, M., Colin, J., Vergnes, J.-P., Alias, A., Saint-Martin, D., Séférian, R., Sénési, S., Voldoire, A., 2019. Recent Changes in the ISBA-CTRIP Land Surface System for Use in the CNRM-CM6 Climate Model and in Global Off-Line Hydrological Applications. J. Adv. Model. Earth Syst. 11, 1207–1252. https://doi.org/10.1029/2018MS001545

Decharme, B., Douville, H., 2006. Introduction of a sub-grid hydrology in the ISBA land surface model. Clim. Dyn. 26, 65–78. https://doi.org/10.1007/s00382-005-0059-7

Devauchelle, O., Petroff, A.P., Seybold, H.F., Rothman, D.H., 2012. Ramification of stream networks. Proc. Natl. Acad. Sci. 109, 20832–20836. https://doi.org/10.1073/pnas.1215218109

Dewandel, B., Boisson, A., Amraoui, N., Caballero, Y., Mougin, B., Baltassat, J.-M., Maréchal, J.-C., 2021. Improving our ability to model crystalline aquifers using field data combined with a regionalized approach for estimating the hydraulic conductivity field. J. Hydrol. 601. https://doi.org/10.1016/j.jhydrol.2021.126652

Dewandel, B., Lachassagne, P., Wyns, R., Maréchal, J.C., Krishnamurthy, N.S., 2006. A generalized 3-D geological and hydrogeological conceptual model of granite aquifers controlled by single or multiphase weathering. J. Hydrol., Hydro-ecological functioning of the Pang and Lambourn catchments, UK 330, 260–284. https://doi.org/10.1016/j.jhydrol.2006.03.026

Dunne, T., Black, R.D., 1970. An Experimental Investigation of Runoff Production in Permeable Soils. Water Resour. Res. 6, 478–490. https://doi.org/10.1029/WR006i002p00478

Dupas, R., Ehrhardt, S., Musolff, A., Fovet, O., Durand, P., 2020. Long-term nitrogen retention and transit time distribution in agricultural catchments in western France. Environ. Res. Lett. 15. https://doi.org/10.1088/1748-9326/abbe47

Durand, Y., Brun, E., Merindol, L., Guyomarc'h, G., Lesaffre, B., Martin, E., 1993. A meteorological estimation of relevant parameters for snow models. Ann. Glaciol. 18, 65–71. https://doi.org/10.3189/S0260305500011277

Famiglietti, J.S., 2014. The global groundwater crisis. Nat. Clim. Change 4, 945–948. https://doi.org/10.1038/nclimate2425

Fan, Y., 2015. Groundwater in the Earth's critical zone: Relevance to large-scale patterns and processes. Water Resour. Res. 51, 3052–3069. https://doi.org/10.1002/2015WR017037

Fan, Y., Bras, R.L., 1998. Analytical solutions to hillslope subsurface storm flow and saturation overland flow. Water Resour. Res. 34, 921–927. https://doi.org/10.1029/97WR03516

Fan, Y., Clark, M., Lawrence, D.M., Swenson, S., Band, L.E., Brantley, S.L., Brooks, P.D., Dietrich, W.E., Flores, A., Grant, et al., 2019. Hillslope Hydrology in Global Change Research and Earth System Modeling. Water Resour. Res. 55, 1737–1772. https://doi.org/10.1029/2018WR023903

Fangmann, A., Haberlandt, U., 2019. Statistical approaches for identification of low-flow drivers: temporal aspects. Hydrol. Earth Syst. Sci. 23, 447–463. https://doi.org/10.5194/hess-23-447-2019

Faroux, S., Kaptué Tchuenté, A.T., Roujean, J.-L., Masson, V., Martin, E., Le Moigne, P., 2013. ECOCLIMAP-II/Europe: a twofold database of ecosystems and surface parameters at 1 km

resolution based on satellite information for use in land surface, meteorological and climate models. Geosci. Model Dev. 6, 563–582. https://doi.org/10.5194/gmd-6-563-2013

Floriancic, M.G., Spies, D., van Meerveld, I.H.J., Molnar, P., 2022. A multi-scale study of the dominant catchment characteristics impacting low-flow metrics. Hydrol. Process. 36. https://doi.org/10.1002/hyp.14462

Franks, S.W., Gineste, P., Beven, K.J., Merot, P., 1998. On constraining the predictions of a distributed model: The incorporation of fuzzy estimates of saturated areas into the calibration process. Water Resour. Res. 34, 787–797. https://doi.org/10.1029/97WR03041

Gascuel-Odoux, C., Weiler, M., Molenat, J., 2010. Effect of the spatial distribution of physical aquifer properties on modelled water table depth and stream discharge in a headwater catchment. Hydrol. Earth Syst. Sci. 14, 1179–1194. https://doi.org/10.5194/hess-14-1179-2010

Gauthier, M.J., Camporese, M., Rivard, C., Paniconi, C., Larocque, M., 2009. A modeling study of heterogeneity and surface water-groundwater interactions in the Thomas Brook catchment, Annapolis Valley (Nova Scotia, Canada). Hydrol. Earth Syst. Sci. 13, 1583–1596. https://doi.org/10.5194/hess-13-1583-2009

Gburek, W.J., Folmar, G.J., 1999. Patterns of contaminant transport in a layered fractured aquifer. J. Contam. Hydrol. 37, 87–109. https://doi.org/10.1016/S0169-7722(98)00158-2

Giorgi, F., Francisco, R., Pal, J., 2003. Effects of a Subgrid-Scale Topography and Land Use Scheme on the Simulation of Surface Climate and Hydrology. Part I: Effects of Temperature and Water Vapor Disaggregation. J. Hydrometeorol. 4, 317–333. https://doi.org/10.1175/1525-7541(2003)4<317:EOASTA>2.0.CO;2

Glaser, B., Antonelli, M., Chini, M., Pfister, L., Klaus, J., 2018. Technical note: Mapping surface-saturation dynamics with thermal infrared imagery. Hydrol. Earth Syst. Sci. 22, 5987–6003. https://doi.org/10.5194/hess-22-5987-2018

Glaser, B., Antonelli, M., Hopp, L., Klaus, J., 2020. Intra-catchment variability of surface saturation – insights from physically based simulations in comparison with biweekly thermal infrared image observations. Hydrol. Earth Syst. Sci. 24, 1393–1413. https://doi.org/10.5194/hess-24-1393-2020

Gleeson, T., Manning, A.H., 2008. Regional groundwater flow in mountainous terrain: Three-dimensional simulations of topographic and hydrogeologic controls. Water Resour. Res. 44. https://doi.org/10.1029/2008WR006848

Gleeson, T., Marklund, L., Smith, L., Manning, A.H., 2011a. Classifying the water table at regional to continental scales. Geophys. Res. Lett. 38. https://doi.org/10.1029/2010GL046427

Gleeson, T., Moosdorf, N., Hartmann, J., van Beek, L.P.H., 2014. A glimpse beneath earth's surface: GLobal HYdrogeology MaPS (GLHYMPS) of permeability and porosity. Geophys. Res. Lett. 41, 3891–3898. https://doi.org/10.1002/2014GL059856

Gleeson, T., Novakowski, K., Kurt Kyser, T., 2009. Extremely rapid and localized recharge to a fractured rock aquifer. J. Hydrol. 376, 496–509. https://doi.org/10.1016/j.jhydrol.2009.07.056

Gleeson, T., Smith, L., Moosdorf, N., Hartmann, J., Dürr, H.H., Manning, A.H., Beek, L.P.H. van, Jellinek, A.M., 2011b. Mapping permeability over the surface of the Earth. Geophys. Res. Lett. 38. https://doi.org/10.1029/2010GL045565

Guillocheau, F., Brault, N., Proust, J.-N., Wyns, R., Thomas, E., Barbarand, J., Bonnet, S., Bourquin, S., Esteoule-Choux, J., Guennoc, et al., 2003. Histoire géologique du Massif Armoricain depuis 140 MA (Crétacé-Actuel) [Geological History of the Armorican Massif since 140 My (Cretaceous-Current)]. Bull Inf. Géol Bassin Paris 40, 13–28.

Habets, F., Boone, A., Champeaux, J.L., Etchevers, P., Franchistéguy, L., Leblois, E., Ledoux, E., Moigne, P.L., Martin, E., Morel, et al., Viennot, P., 2008. The SAFRAN-ISBA-MODCOU hydrometeorological model applied over France. J. Geophys. Res. Atmospheres 113. https://doi.org/10.1029/2007JD008548

Habets, F., Etchevers, P., Golaz, C., Leblois, E., Ledoux, E., Martin, E., Noilhan, J., Ottlé, C., 1999. Simulation of the water budget and the river flows of the Rhone basin. J. Geophys. Res. Atmospheres 104, 31145–31172. https://doi.org/10.1029/1999JD901008

Haitjema, H.M., Mitchell-Bruker, S., 2005. Are Water Tables a Subdued Replica of the Topography? Groundwater 43, 781–786. https://doi.org/10.1111/j.1745-6584.2005.00090.x

Harman, C.J., Sivapalan, M., Kumar, P., 2009. Power law catchment-scale recessions arising from heterogeneous linear small-scale dynamics. Water Resour. Res. 45. https://doi.org/10.1029/2008WR007392

Hartmann, A., 2016. Putting the cat in the box: why our models should consider subsurface heterogeneity at all scales. WIREs Water 3, 478–486. https://doi.org/10.1002/wat2.1146

Hartmann, A., Gleeson, T., Wada, Y., Wagener, T., 2017. Enhanced groundwater recharge rates and altered recharge sensitivity to climate variability through subsurface heterogeneity. Proc. Natl. Acad. Sci. 114, 2842–2847. https://doi.org/10.1073/pnas.1614941114

He, X., Stisen, S., Wiese, M.B., Henriksen, H.J., 2016. Designing a Hydrological Real-Time System for Surface Water and Groundwater in Denmark with Engagement of Stakeholders. Water Resour. Manag. 30, 1785–1802. https://doi.org/10.1007/s11269-016-1251-8

Henriksen, H.J., Troldborg, L., Nyegaard, P., Sonnenborg, T.O., Refsgaard, J.C., Madsen, B., 2003. Methodology for construction, calibration and validation of a national hydrological model for Denmark. J. Hydrol. 280, 52–71. https://doi.org/10.1016/S0022-1694(03)00186-0

Hewlett, J.D., Hibbert, A.R., 1967. Factors affecting the response of small watersheds to precipitation in humid areas. For. Hydrol. 33, 275–290. https://doi.org/10.1177/0309133309338118

Hilberts, A.G.J., van Loon, E.E., Troch, P.A., Paniconi, C., 2004. The hillslope-storage Boussinesq model for non-constant bedrock slope. J. Hydrol. 291, 160–173. https://doi.org/10.1016/j.jhydrol.2003.12.043

Hyun, Y., Kim, H., Lee, S.-S., Lee, K.-K., 2011. Characterizing streambed water fluxes using temperature and head data on multiple spatial scales in Munsan stream, South Korea. J. Hydrol. 402, 377–387. https://doi.org/10.1016/j.jhydrol.2011.03.032

Jachens, E.R., Rupp, D.E., Roques, C., Selker, J.S., 2020. Recession analysis revisited: impacts of climate on parameter estimation. Hydrol. Earth Syst. Sci. 24, 1159–1170. https://doi.org/10.5194/hess-24-1159-2020

Kirchner, J.W., 2009. Catchments as simple dynamical systems: Catchment characterization, rainfall-runoff modeling, and doing hydrology backward. Water Resour. Res. 45. https://doi.org/10.1029/2008WR006912

Kolbe, T., Marçais, J., de Dreuzy, J.-R., Labasque, T., Bishop, K., 2020. Lagged rejuvenation of groundwater indicates internal flow structures and hydrological connectivity. Hydrol. Process. 34, 2176–2189. https://doi.org/10.1002/hyp.13753

Kolbe, T., Marçais, J., Thomas, Z., Abbott, B.W., de Dreuzy, J.-R., Rousseau-Gueutin, P., Aquilina, L., Labasque, T., Pinay, G., 2016. Coupling 3D groundwater modeling with CFC-based age dating to classify local groundwater circulation in an unconfined crystalline aquifer. J. Hydrol. 543, 31–46. https://doi.org/10.1016/j.jhydrol.2016.05.020

Kollet, S.J., Maxwell, R.M., 2006. Integrated surface–groundwater flow modeling: A free-surface overland flow boundary condition in a parallel groundwater flow model. Adv. Water Resour. 29, 945–958. https://doi.org/10.1016/j.advwatres.2005.08.006

Kovács, G., 2011. Seepage Hydraulics. Elsevier.

Krasny, J., 2002. Quantitative hardrock hydrogeology in a regional scale. Geol Surv Nor. Bull 439, 7–14.

Lachassagne, P., Dewandel, B., Wyns, R., 2021. Review: Hydrogeology of weathered crystalline/hard-rock aquifers—guidelines for the operational survey and management of their groundwater resources. Hydrogeol. J. 29, 2561–2594. https://doi.org/10.1007/s10040-021-02339-7

Lafaysse, M., Hingray, B., Etchevers, P., Martin, E., Obled, C., 2011. Influence of spatial discretization, underground water storage and glacier melt on a physically-based hydrological model of the Upper Durance River basin. J. Hydrol. 403, 116–129. https://doi.org/10.1016/j.jhydrol.2011.03.046

Lague, D., Davy, P., Crave, A., 2000. Estimating uplift rate and erodibility from the area-slope relationship: Examples from Brittany (France) and numerical modelling. Phys. Chem. Earth Part Solid Earth Geod. 25, 543–548. https://doi.org/10.1016/S1464-1895(00)00083-1

Lana-Renault, N., Regüés, D., Serrano, P., Latron, J., 2014. Spatial and temporal variability of groundwater dynamics in a sub-Mediterranean mountain catchment. Hydrol. Process. 28, 3288–3299. https://doi.org/10.1002/hyp.9892

Le Borgne, T., Bour, O., de Dreuzy, J.-R., Davy, P., Touchard, F., 2004. Equivalent mean flow models for fractured aquifers: Insights from a pumping tests scaling interpretation. Water Resour. Res. 40. https://doi.org/10.1029/2003WR002436

Le Moigne, P., 2009. SURFEX scientific documentation. Note de centre (CNRM/GMME), available online at: http://www.cnrm.meteo.fr/surfex/, last access: December 2021, Météo-France, CNRM, Toulouse, France 211.

Le Moigne, P., Besson, F., Martin, E., Boé, J., Boone, A., Decharme, B., Etchevers, P., Faroux, S., Habets, F., Lafaysse, et al., 2020. The latest improvements with SURFEX v8.0 of the Safran–Isba–Modcou hydrometeorological model for France. Geosci. Model Dev. 13, 3925–3946. https://doi.org/10.5194/gmd-13-3925-2020

Loritz, R., Hassler, S.K., Jackisch, C., Allroggen, N., van Schaik, L., Wienhöfer, J., Zehe, E., 2017. Picturing and modeling catchments by representative hillslopes. Hydrol. Earth Syst. Sci. 21, 1225–1249. https://doi.org/10.5194/hess-21-1225-2017

Marçais, J., de Dreuzy, J.-R., Erhel, J., 2017. Dynamic coupling of subsurface and seepage flows solved within a regularized partition formulation. Adv. Water Resour. 109, 94–105. https://doi.org/10.1016/j.advwatres.2017.09.008

Martin, C., Molénat, J., Gascuel-Odoux, C., Vouillamoz, J.-M., Robain, H., Ruiz, L., Faucheux, M., Aquilina, L., 2006. Modelling the effect of physical and chemical characteristics of shallow aquifers on water and nitrate transport in small agricultural catchments. J. Hydrol. 326, 25–42. https://doi.org/10.1016/j.jhydrol.2005.10.040

Masson, V., Champeaux, J.-L., Chauvin, F., Meriguet, C., Lacaze, R., 2003. A Global Database of Land Surface Parameters at 1-km Resolution in Meteorological and Climate Models. J. Clim. 16, 1261–1282. https://doi.org/10.1175/1520-0442(2003)16<1261:AGDOLS>2.0.CO;2

Masson, V., Le Moigne, P., Martin, E., Faroux, S., Alias, A., Alkama, R., Belamari, S., Barbu, A., Boone, A., Bouyssel, F., et al., 2013. The SURFEXv7.2 land and ocean surface platform for coupled or offline simulation of earth surface variables and fluxes. Geosci. Model Dev. 6, 929–960. https://doi.org/10.5194/gmd-6-929-2013

Matonse, A.H., Kroll, C., 2009. Simulating low streamflows with hillslope storage models. Water Resour. Res. 45. https://doi.org/10.1029/2007WR006529

Maxwell, R.M., Kollet, S.J., 2008. Interdependence of groundwater dynamics and land-energy feedbacks under climate change. Nat. Geosci. 1, 665–669. https://doi.org/10.1038/ngeo315

Mendoza, G.F., Steenhuis, T.S., Walter, M.T., Parlange, J.-Y., 2003. Estimating basin-wide hydraulic parameters of a semi-arid mountainous watershed by recession-flow analysis. J. Hydrol. 279, 57–69. https://doi.org/10.1016/S0022-1694(03)00174-4

Messager, M.L., Lehner, B., Cockburn, C., Lamouroux, N., Pella, H., Snelder, T., Tockner, K., Trautmann, T., Watt, C., Datry, T., 2021. Global prevalence of non-perennial rivers and streams. Nature 594, 391–397. https://doi.org/10.1038/s41586-021-03565-5

Mougin, B., Allier, D., Blanchin, R., Carn, A., Courtois, N., Gateau, C., Putot, E., 2008. Project SILURES, Final report year 5 BRGM/RP-56457-FR, available online at: https://infoterre.brgm.fr/rapports/RP-56457-FR.pdf, last access: December 2021.

Napoly, A., Boone, A., Samuelsson, P., Gollvik, S., Martin, E., Seferian, R., Carrer, D., Decharme, B., Jarlan, L., 2017. The interactions between soil–biosphere–atmosphere (ISBA) land surface model multi-energy balance (MEB) option in SURFEXv8 – Part 2: Introduction of a litter formulation and model evaluation for local-scale forest sites. Geosci. Model Dev. 10, 1621–1644. https://doi.org/10.5194/gmd-10-1621-2017

Nash, J.E., Sutcliffe, J.V., 1970. River flow forecasting through conceptual models part I — A discussion of principles. J. Hydrol. 10, 282–290. https://doi.org/10.1016/0022-1694(70)90255-6

Noilhan, J., Planton, S., 1989. A Simple Parameterization of Land Surface Processes for Meteorological Models. Mon. Weather Rev. 117, 536–549. https://doi.org/10.1175/1520-0493(1989)117<0536:ASPOLS>2.0.CO;2

Ogden, F.L., Watts, B.A., 2000. Saturated area formation on nonconvergent hillslope topography with shallow soils: A numerical investigation. Water Resour. Res. 36, 1795–1804. https://doi.org/10.1029/2000WR900091

Paniconi, C., Putti, M., 2015. Physically based modeling in catchment hydrology at 50: Survey and outlook. Water Resour. Res. 51, 7090–7129. https://doi.org/10.1002/2015WR017780

Paniconi, C., Troch, P.A., Loon, E.E. van, Hilberts, A.G.J., 2003. Hillslope-storage Boussinesq model for subsurface flow and variable source areas along complex hillslopes: 2. Intercomparison with a three-dimensional Richards equation model. Water Resour. Res. 39. https://doi.org/10.1029/2002WR001730

Parlange, J.-Y., Stagnitti, F., Heilig, A., Szilagyi, J., Parlange, M.B., Steenhuis, T.S., Hogarth, W.L., Barry, D.A., Li, L., 2001. Sudden drawdown and drainage of a horizontal aquifer. Water Resour. Res. 37, 2097–2101. https://doi.org/10.1029/2000WR000189

Perrin, C., Michel, C., Andréassian, V., 2001. Does a large number of parameters enhance model performance? Comparative assessment of common catchment model structures on 429 catchments. J. Hydrol. 242, 275–301. https://doi.org/10.1016/S0022-1694(00)00393-0

Price, K., 2011. Effects of watershed topography, soils, land use and climate on baseflow hydrology in humid regions: a review. Prog. Physcial Geogr. 35, 465–492. https://doi.org/10.1177/0309133311402714

Quintana-Seguí, P., Le Moigne, P., Durand, Y., Martin, E., Habets, F., Baillon, M., Canellas, C., Franchisteguy, L., Morel, S., 2008. Analysis of Near-Surface Atmospheric Variables: Validation of the SAFRAN Analysis over France. J. Appl. Meteorol. Climatol. 47, 92–107. https://doi.org/10.1175/2007JAMC1636.1

Raimonet, M., Oudin, L., Thieu, V., Silvestre, M., Vautard, R., Rabouille, C., Le Moigne, P., 2017. Evaluation of Gridded Meteorological Datasets for Hydrological Modeling. J. Hydrometeorol. 18, 3027–3041. https://doi.org/10.1175/JHM-D-17-0018.1

Reynolds, D.R., Gardner, D.J., Balos, C.J., Woodward, C.S., 2019. SUNDIALS Multiphysics+MPIManyVector Performance Testing.

Riebe, C.S., Hahm, W.J., Brantley, S.L., 2017. Controls on deep critical zone architecture: a historical review and four testable hypotheses. Earth Surf. Process. Landf. 42, 128–156. https://doi.org/10.1002/esp.4052

Ritter, A., Muñoz-Carpena, R., 2013. Performance evaluation of hydrological models: Statistical significance for reducing subjectivity in goodness-of-fit assessments. J. Hydrol. 480, 33–45. https://doi.org/10.1016/j.jhydrol.2012.12.004

Roques, C., Aquilina, L., Bour, O., Maréchal, J.-C., Dewandel, B., Pauwels, H., Labasque, T., Vergnaud-Ayraud, V., Hochreutener, R., 2014. Groundwater sources and geochemical processes in a crystalline fault aquifer. J. Hydrol. 519, 3110–3128. https://doi.org/10.1016/j.jhydrol.2014.10.052

Roques, C., Bour, O., Aquilina, L., Dewandel, B., 2016. High-yielding aquifers in crystalline basement: insights about the role of fault zones, exemplified by Armorican Massif, France. Hydrogeol. J. 24, 2157–2170. https://doi.org/10.1007/s10040-016-1451-6

Schwanghart, W., Kuhn, N.J., 2010. TopoToolbox: A set of Matlab functions for topographic analysis. Environ. Model. Softw. 25, 770–781. https://doi.org/10.1016/j.envsoft.2009.12.002

Singhal, B.B.S., Gupta, R.P., 2010. Applied Hydrogeology of Fractured Rocks: Second Edition. Springer Science & Business Media.

Sophocleous, M., 2002. Interactions between groundwater and surface water: the state of the science. Hydrogeol. J. 10, 52–67. https://doi.org/10.1007/s10040-001-0170-8

St. Clair, J., Moon, S., Holbrook, W.S., Perron, J.T., Riebe, C.S., Martel, S.J., Carr, B., Harman, C., Singha, K., Richter, D. et al., 2015. Geophysical imaging reveals topographic stress control of bedrock weathering. Science 350, 534–538. https://doi.org/10.1126/science.aab2210

Staudinger, M., Stoelzle, M., Cochand, F., Seibert, J., Weiler, M., Hunkeler, D., 2019. Your work is my boundary condition!: Challenges and approaches for a closer collaboration between hydrologists and hydrogeologists. J. Hydrol. 571, 235–243. https://doi.org/10.1016/j.jhydrol.2019.01.058

Sulis, M., Meyerhoff, S.B., Paniconi, C., Maxwell, R.M., Putti, M., Kollet, S.J., 2010. A comparison of two physics-based numerical models for simulating surface water–groundwater interactions. Adv. Water Resour. 33, 456–467. https://doi.org/10.1016/j.advwatres.2010.01.010

Tashie, A., Pavelsky, T., Band, L.E., 2020a. An Empirical Reevaluation of Streamflow Recession Analysis at the Continental Scale. Water Resour. Res. 56. https://doi.org/10.1029/2019WR025448

Tashie, A., Pavelsky, T., Emanuel, R.E., 2020b. Spatial and Temporal Patterns in Baseflow Recession in the Continental United States. Water Resour. Res. 56. https://doi.org/10.1029/2019WR026425

Tashie, A., Scaife, C.I., Band, L.E., 2019. Transpiration and subsurface controls of streamflow recession characteristics. Hydrol. Process. 33, 2561–2575. https://doi.org/10.1002/hyp.13530

Taylor, R., Howard, K., 2000. A tectono-geomorphic model of the hydrogeology of deeply weathered crystalline rock: Evidence from Uganda. Hydrogeol. J. 8, 279–294. https://doi.org/10.1007/s100400000069

Thomas, Z., Ghazavi, R., Merot, P., Granier, A., 2012. Modelling and observation of hedgerow transpiration effect on water balance components at the hillslope scale in Brittany. Hydrol. Process. 26, 4001–4014. https://doi.org/10.1002/hyp.9198

Troch, P.A., Berne, A., Bogaart, P., Harman, C., Hilberts, A.G.J., Lyon, S.W., Paniconi, C., Pauwels, V.R.N., Rupp, D.E., Selker, J.S., et al., 2013. The importance of hydraulic groundwater theory in catchment hydrology: The legacy of Wilfried Brutsaert and Jean-Yves Parlange. Water Resour. Res. 49, 5099–5116. https://doi.org/10.1002/wrcr.20407

Troch, P.A., De Troch, F.P., Brutsaert, W., 1993. Effective water table depth to describe initial conditions prior to storm rainfall in humid regions. Water Resour. Res. 29, 427–434. https://doi.org/10.1029/92WR02087

Troch, P.A., Paniconi, C., Loon, E.E. van, 2003. Hillslope-storage Boussinesq model for subsurface flow and variable source areas along complex hillslopes: 1. Formulation and characteristic response. Water Resour. Res. 39. https://doi.org/10.1029/2002WR001728

Van Loon, A.F., Laaha, G., 2015. Hydrological drought severity explained by climate and catchment characteristics. J. Hydrol., Drought processes, modeling, and mitigation 526, 3–14. https://doi.org/10.1016/j.jhydrol.2014.10.059

Vannier, O., Braud, I., Anquetin, S., 2014. Regional estimation of catchment-scale soil properties by means of streamflow recession analysis for use in distributed hydrological models. Hydrol. Process. 28, 6276–6291. https://doi.org/10.1002/hyp.10101

Vergnes, J.-P., Decharme, B., Habets, F., 2014. Introduction of groundwater capillary rises using subgrid spatial variability of topography into the ISBA land surface model. J. Geophys. Res. Atmospheres 119, 11,065-11,086. https://doi.org/10.1002/2014JD021573

Vergnes, J.-P., Roux, N., Habets, F., Ackerer, P., Amraoui, N., Besson, F., Caballero, Y., Courtois, Q., de Dreuzy, J.-R., Etchevers, P., et al., 2020a. The AquiFR hydrometeorological modelling platform as

a tool for improving groundwater resource monitoring over France: evaluation over a 60-year period. Hydrol. Earth Syst. Sci. 24, 633–654. https://doi.org/10.5194/hess-24-633-2020

Vidal, J.-P., Martin, E., Franchistéguy, L., Baillon, M., Soubeyroux, J.-M., 2010. A 50-year high-resolution atmospheric reanalysis over France with the Safran system. Int. J. Climatol. 30, 1627–1644. https://doi.org/10.1002/joc.2003

Vincendon, B., Ducrocq, V., Saulnier, G.-M., Bouilloud, L., Chancibault, K., Habets, F., Noilhan, J., 2010. Benefit of coupling the ISBA land surface model with a TOPMODEL hydrological model version dedicated to Mediterranean flash-floods. J. Hydrol., Flash Floods: Observations and Analysis of Hydrometeorological Controls 394, 256–266. https://doi.org/10.1016/j.jhydrol.2010.04.012

Widory, D., Kloppmann, W., Chery, L., Bonnin, J., Rochdi, H., Guinamant, J.-L., 2004. Nitrate in groundwater: an isotopic multi-tracer approach. J. Contam. Hydrol. 72, 165–188. https://doi.org/10.1016/j.jconhyd.2003.10.010

Wittenberg, H., 1999. Baseflow recession and recharge as nonlinear storage processes. Hydrol. Process. 13, 715–726. https://doi.org/10.1002/(SICI)1099-1085(19990415)13:5<715::AID-HYP775>3.0.CO;2-N

Worthington, S.R.H., Davies, G.J., Alexander, E.C., 2016. Enhancement of bedrock permeability by weathering. Earth-Sci. Rev. 160, 188–202. https://doi.org/10.1016/j.earscirev.2016.07.002

Wright, E.P., Burgess, W.G., 1992. The hydrogeology of crystalline basement aquifers in Africa. pp. 1–27.

Wyns, R., Baltassat, J.-M., Lachassagne, P., Legchenko, A., Vairon, J., Mathieu, F., 2004. Application of proton magnetic resonance soundings to groundwater reserve mapping in weathered basement rocks (Brittany, France). Bull. Société Géologique Fr. 175, 21–34. https://doi.org/10.2113/175.1.21

Xiao, D., Shi, Y., Brantley, S.L., Forsythe, B., DiBiase, R., Davis, K., Li, L., 2019. Streamflow Generation From Catchments of Contrasting Lithologies: The Role of Soil Properties, Topography, and Catchment Size. Water Resour. Res. 55, 9234–9257. https://doi.org/10.1029/2018WR023736

Yu, D., Lane, S.N., 2011. Interactions between subgrid-scale resolution, feature representation and grid-scale resolution in flood inundation modelling. Hydrol. Process. 25, 36–53. https://doi.org/10.1002/hyp.7813

APPENDICES

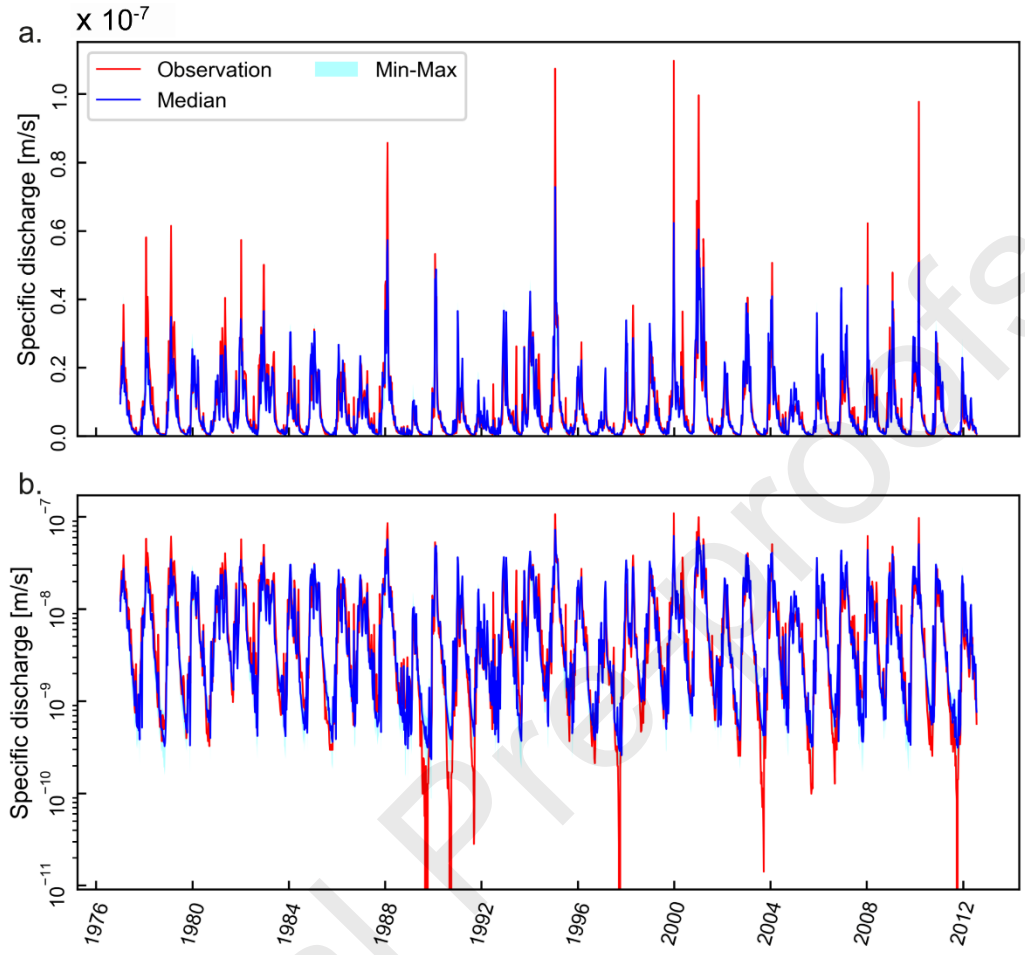

Fig. A.1. Results and performances of the calibrated models for the 1970-2012 period for the Arguenon catchment in linear scale (a) and logarithmic scale (b). Red and blue curves display observed and modeled specific discharge timeseries. Cyan area shows the variability of modeled specific discharge.

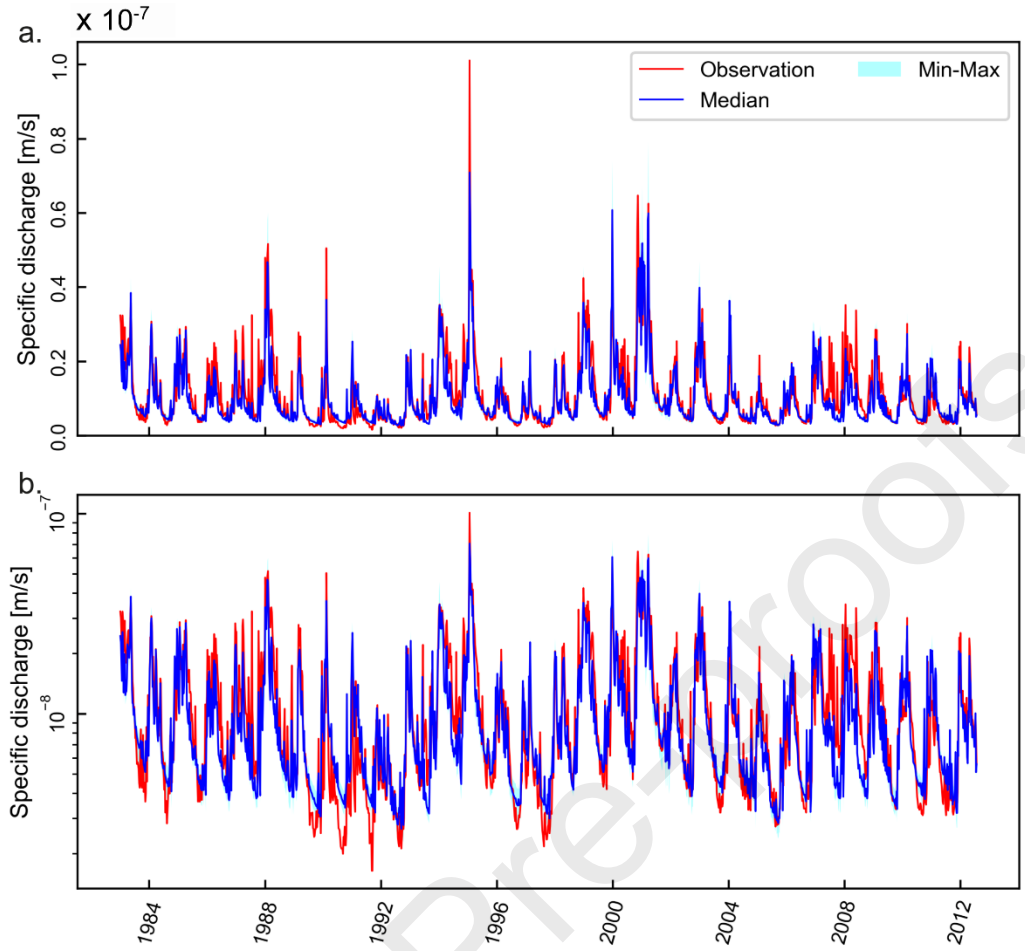

Fig. A.2. Results and performances of the calibrated models for the 1970-2012 period for the Nançon catchment in linear scale (a) and logarithmic scale (b). Red and blue curves display observed and modeled specific discharge timeseries. Cyan area shows the variability of modeled specific discharge.

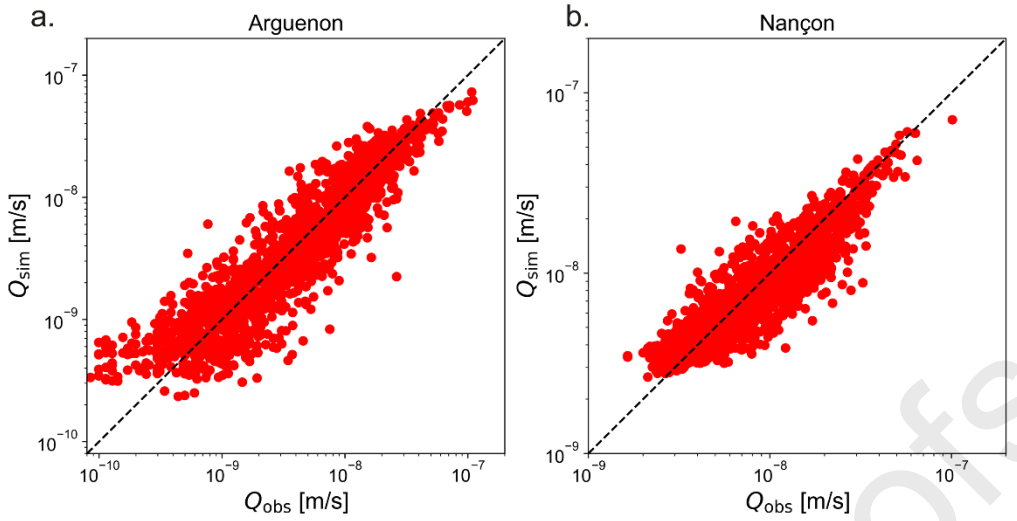

Fig. A.3. Results and performances of the calibrated models for the 1970-2012. Dark dashed curves represent a perfect fit between simulted and observed discharges (Q_{sim} and Q_{obs}). Red points display the fit between these data at each point of the discharge timeseries.

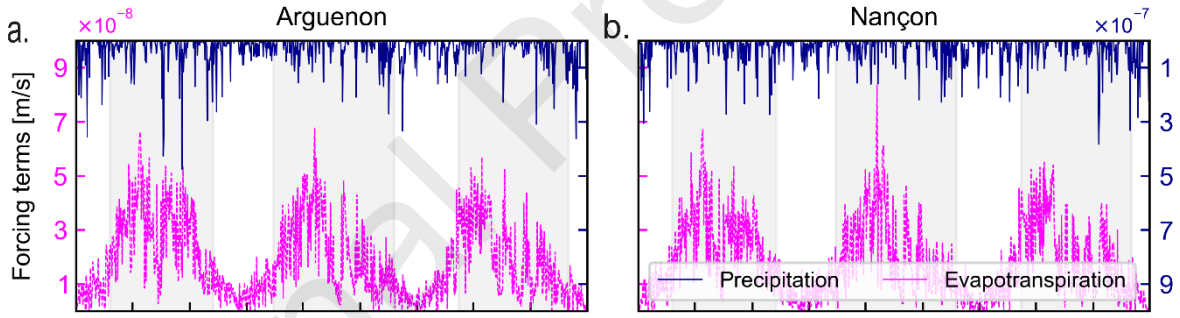

Fig. A.4. Precipitation and evapotranspiration timeseries for the 2004-2006 period. Left and right columns represent respectively the results for the Arguenon and Nançon catchments. The successive grey and white bands underline the overall recession period from April to October and recharge period from November to March. a) and b) show the precipitation timeseries and the evapotranspiration given by the SURFEX hydrometeorological model.

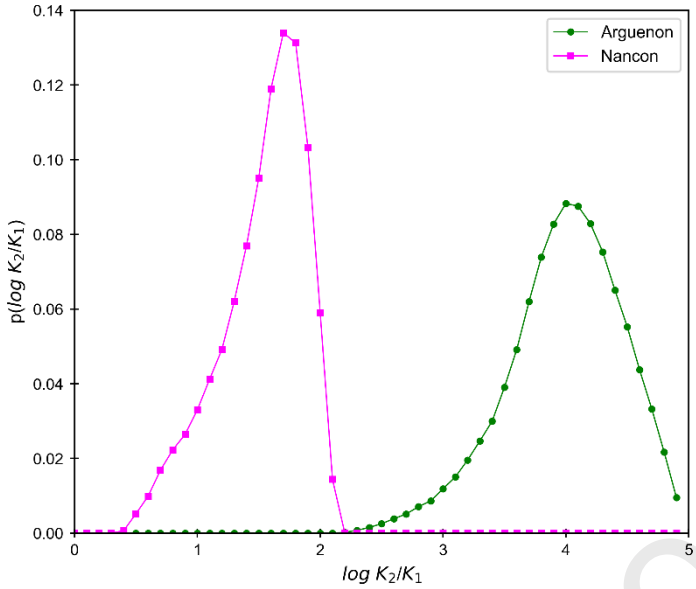

Fig. A.3. Distribution of hydraulic conductivity ratio between the two equivalent hillslopes for the Arguenon (fuchsia line) and Nançon (green line) catchments. Note that $K_2>K_1$ and $log(K_2/K_1)>0$.

- Groundwater-surface water interactions are studied in two shallow aquifers
- A combination of hillslope processes shapes the catchment-scale streamflows.
- Low-conductive hillslopes enhance overland flows and sustain late recessions.
- High-diffusive hillslopes shape the event- and seasonal-scale recessions.
- Hydraulic properties are significantly heterogeneous at the catchment scale